Quantitative Evaluation of DC Microgrids Availability: Effects of System Architecture and Converter Topology Design Choices

Alexis Kwasinski, *Member, IEEE*

Abstract—This paper presents a quantitative method to evaluate dc microgrids availability by identifying and calculating minimum cut sets occurrence probability for different microgrid architectures and converter topologies. Hence, it provides planners with an essential tool to evaluate downtime costs and decide technology deployments based on quantitative risk assessments by allowing to compare the effect that converter topologies and microgrid architecture choices have on availability. Conventional architectures with single-input converters and alternative configurations with multiple-input converters (MICs) are considered. Calculations yield that all microgrid configurations except those utilizing center converters achieve similar availability of 6-nines. Three converter topologies are used as representatives of many other circuits. These three benchmark circuits are the boost, the isolated SEPIC (ISEPIC), and the current-source half-bridge. Marginal availability differences are observed for different circuit topology choices, although architectures with MICs are more sensitive to this choice. MICs and, in particular, the ISEPIC, are identified as good compromise options for dc microgrids source interfaces. The analysis also models availability influence of local energy storage, both in batteries and generators' fuel. These models provide a quantitative way of comparing dc microgrids with conventional backup energy systems. Calculations based on widely accepted data in industry supports the analysis.

Index Terms—Availability, converters, dc–dc power conversion, dc power systems, diversity methods, microgrids, planning, power electronics.

I. INTRODUCTION

THIS paper presents an availability calculation method for microgrids that is used to explore how dc microgrids availability is affected by the different circuit topology design choices for the power electronic interfaces between the distributed generation (DG) sources and the rest of the microgrid. The influence of alternative system architectures on availability is also evaluated. The ultimate goal is to gain insights on microgrid availability characteristics that will facilitate the design of ultra-available power plants for critical loads, such as data centers [1],

communication sites [2], hospitals, and security facilities. Thus, the focus is on dc systems because statistical operational data comparing ac and dc systems for critical loads show that dc architectures have an availability at least two orders or magnitude higher than that of ac systems [3]. Moreover, dc is chosen over ac because it facilitates integrating most modern electronic loads, energy storage devices, and DG technologies—all of them inherently dc.

One of the claimed potential microgrid advantages is their improved local power availability with respect to that of the electric grid, of about 0.999 (or as it is usually termed 3-nines) [4], or to that of conventional backup plants with standby generators and no energy storage, of about 4-nines [5], [6]. However, most DG technologies have generation units with availabilities at best of about 2-nines [6]. Thus, improved local availability can only be achieved by having diverse power sources in redundant architectures, or by adding energy storage. Yet, the latter option is often the alternative that is attempted to be avoided through microgrids with DG sources [7], [8]. Thus, adequate microgrid designs need to consider power electronic interfaces suitable to integrate sources of various technologies, which imply that availability analysis cannot be decoupled from understanding the role that converter circuit topologies and system architectures play on microgrids availability.

Typically, most past conventional evaluations of microgrids focus among some of its advantages on evaluating emissions [9], costs [9]–[13], or fuel consumption [13], [14]. Although these are important aspects that deserve to be the focus of attention of the scientific community, another potential advantage of microgrids, high availability, seem to not have received as much formal attention. In past works, high availability is often mentioned as one of the main microgrids technical advantages [9] [15]–[27], but many of these past works [15]–[19] do not provide proof to this claim and most of the rest of these works explore reliability by considering microgrids small conventional power grids [20]–[24]. Thus, their approach follows convention power flow approximations without quantifying failure probabilities, considering failure and repair rates, or even without including any power electronic interfaces [20]–[24]. A similar approach is observed in [9] in which reliability is examined from an operational perspective by studying matching generation and loads, and by considering perfect reliable components. Still, there are few works exploring how power electronic interfaces design affect microgrids availability, or that present availability calculation models and methods for dc microgrids. One of these past works considers availability mainly from an energy supply

perspective [25], but still recognize some of the conventional availability improving techniques, such as redundancy and modularity. Another of these works compares power electronic interfaces for dc microgrids [26] based on different criteria, but the analysis is qualitative, focuses only on one type of interfaces—multiple-input converters (MICs)—and concentrates on reliability, not system availability. Yet another work [27] explored availability issues, but the focus was on circuit analysis of a particular MIC topology. In addition to MICs, the study presented here includes evaluation of system architectures with conventional single-input converter (SIC) topologies [15], [28], [29].

This paper contributes to the field of stationary power electronics applications and, in particular, microgrids by presenting a novel framework that calculates dc microgrids availability based on minimal cut sets (mcs) theory. Application of this availability calculation method is explained in detail by quantitatively evaluating microgrids availability advantages and examining how these advantages are affected by design choices. The effect of converter circuit design on system availability is assessed with calculations based on three dc–dc converter topologies—boost, isolated SEPIC (ISEPIC), and current-source half-bridge (CSHB)—that are taken as benchmarks because they are representative of most other circuit topologies. This discussion addressed meaningful questions of dc microgrids planning and design that for the most part have not been sufficiently treated in the literature, such as whether or not MICs may yield better availability than SICs as implied in [30] and [31]. Also, what is the difference in availability when using MICs when compared to that of SICs? How much difference there is in availability for various microgrid architectures? Since some previous works indicate without providing a detailed assessment that dc microgrids may achieve higher availability than conventional backup energy systems—e.g. telecom energy systems—intended for highly available power supply [2], [6]–[8] in which at least 5 or 6-nines availability is required [32], [33], other topics discussed in here include answers to other relevant questions, such as how dc microgrids compare in terms of availability with respect to conventional backup plants. In this sense, how much energy storage is required in conventional backup systems in order to reach availabilities similar to that of microgrids?

The quantitative analytical approach presented here is essential in order to provide useful information for planning, configuring, and operating microgrids. For example, availability values provided here can be used in quantitative risk assessments that allow evaluating downtime costs with respect to system capital and operational costs in order to determine the most appropriate technological solution in a given application [34]. The presented calculation method could also be integrated within a microgrid advanced controller in order to provide a continuous real-time system availability estimate; therefore, the microgrid can be operated at a maximum availability mode. Inputs to this controller may include site environmental data—e.g., condition of the fuel supply system or critical components temperature—or historical failure data from the same site and other equivalent sites in order to dynamically adjust failure rates in real time. The analysis can be somewhat automated and adapted to alternative configurations than those used here by realizing that architecture

blocks with similar arrangements lead to similar mcs. A way to evaluate the impact of locally stored energy is also detailed in this paper and this quantitative assessment of locally added energy storage is used to detail a mean to compare microgrids availability performance to that of conventional backup energy systems. Finally, a related contribution to the knowledge base in highly available power electronics systems is also included in this paper by deriving a form to calculate conventional standby energy plants unavailability, considering the effect of locally stored fuel. The analysis is supported by calculations based on reliability data widely accepted in industry.

II. PRELIMINARY NOTIONS

A. Reliability and Availability Analysis

Since microgrids are repairable systems that are intended to operate continuously or that may still be considered operational even when one or more components fail, availability can be defined both as the probability that the microgrid is providing full power to the load at any given time t, or as the expected portion of the time that the microgrid performs its required function—i.e., powering the load. Mathematically, this definition of availability implies that

$$A = \frac{\mu}{\lambda + \mu} = \frac{T_U}{T_U + T_D} \qquad (1)$$

where A is the availability, μ and λ are the microgrid's repair and failure rates, respectively, and T_U and T_D are its mean up time (MUT) and mean down time (MDT), respectively. The mean time between failures (MTBF) is, then, $T_U + T_D$, and μ and λ are the inverse of the MDT and MUT, respectively. Unavailability U is defined as $1 - A$. Although the concept of availability is similar to the concept of reliability, they both should not be confused. Availability is a concept that builds on the concept of reliability. In terms of a quantitative measure the reliability of some entity is defined as the probability that a particular entity under consideration works meeting some operational goals under given conditions for a given time interval [35]. This definition is based on the implicit assumption that a reliability test is made with the entity separated from any other potentially interacting entity. In this implicit assumption lies a fundamental difference between the concepts of reliability and availability. Whereas reliability applies to independent entities, availability applies to entities that interact with other entities and/or that are influenced by external factors not directly related with any physical interaction within the system, such as maintenance policies. For this reason, the concept of reliability applies to separable components or entities, such as a circuit, whereas availability is applicable to systems formed by a number or components. Hence, availability is not only influenced by its components reliability behavior, but also by how those components interact among themselves—e.g., how they are interconnected to form the system architecture—how the system is configured—e.g., whether or not there are redundant components—or what are the maintenance policies—e.g., whether or not spares are kept at the site in order to reduce the MDT—among other influencing factors. Thus, the definition of availability of an entity or system

considers its forming components by the function they perform and not necessarily by their physical constitution or existence. However, the definition of reliability refers to the physical entity that is under consideration. For this reason, the concept of reliability applies to system components that cannot be repaired, so when this particular component fails, although it may still be possible to be replaced into the system by another component performing the same function, the failed component itself, as a separate entity for which reliability is assessed, can no longer be repaired. Hence, when calculating reliability, the concept of MTBF shall be replaced by that of mean time to failure (MTTF).

This distinction between the concept of reliability that applies to separable physical entities and that of availability that applies primarily to systems or entities in which its components are viewed primarily by the function they perform, motivates some techniques to improve availability. Among these techniques used to improve availability, two that are relevant for the analysis conducted in here are redundancy—to have more than the minimum needed number of a given component performing the same function—and diversity—to have different system components that can perform the same function. A well-designed microgrid with a redundant and/or diverse design can sustain failures in one or more of its components, while it is still able to fully power the load. The possibility that a system can still meet its operational goals when one or more of its components fail is another characteristic that differentiates the use of the concept of availability and reliability. For the latter, the notion of operation within specifications even when there are failures present is not applicable. Modular designs also contribute to improve system availability by allowing a small ratio of the MDT to the MTBF through fast replacement of failed components [36]. Without a modular design, redundant configurations cannot be implemented [37]. The opposing alternative to a modular architecture is termed as a centralized design [28].

B. Reference Converter Topologies

Since most DG technologies inherently produce dc power, there are two basic families of converters that can be used to integrate these local generation units into a common main system bus to form a dc microgrid. One, exemplified in Fig. 1 is the conventional approach of using SICs. The other, exemplified in Fig. 2 is to use MICs. MICs are typically realized by taking a conventional SIC and splitting its circuit into a common output stage and an input stage that is replicated in order to produce one input for each replicated original input stage. Hence, MICs tend to facilitate integrating various sources. Some of the past studies that describe alternative ways of realizing MICs are [38]–[41]. Although some previous works on MICs claim without proof that they can achieve higher reliability [30], [31], it is not clear how this characteristic can be verified considering that the common output stage may act as a single point of failure for all sources connected to that same MIC module, thus, negating the advantage of having diverse inputs. For this reason, it is relevant to quantitatively evaluate how MIC design affects microgrids availability.
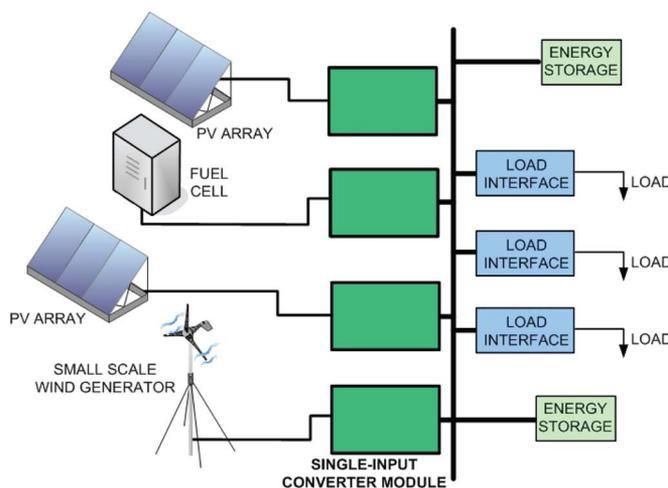

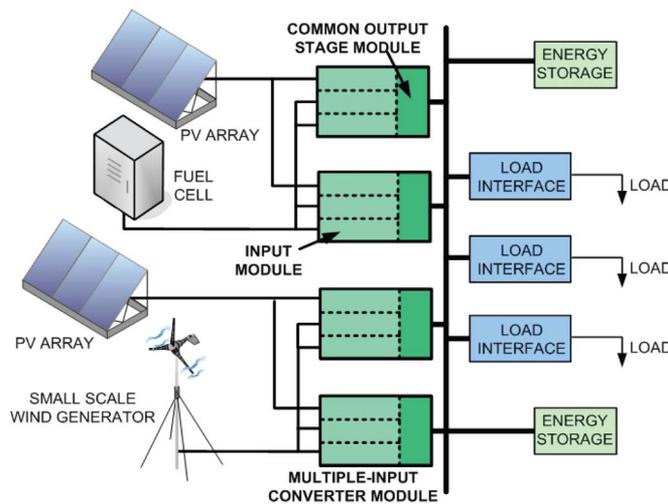Fig. 1. Possible dc microgrid architecture with SICs.

Fig. 2. Possible dc microgrid architecture with MICs.

Fig. 3 shows three of the most general ways in which MICs can be realized depending on the connection point among input modules [26] and one example of a representative circuit topology for each case. The simplest approach is to make all inputs to share only the output capacitor, as in the MI boost [42]. Yet, this approach, shown in Fig. 3(a), is only arguably a MIC because it can also be considered a parallel connection of boost converters in which the output capacitor of each boost converter is replaced by a single capacitor. Another option is to link all inputs magnetically at a common magnetic core, as shown in the MI CSHB [40] in Fig. 3(b). The third option, displayed in Fig. 3(c) and exemplified with a MI ISEPIC [43], is to make the input modules to share at least one uncontrolled switch and a capacitor and possibly an inductor or coupled inductors. Since these three dc–dc converter topologies—boost, ISEPIC, and CSHB—are representative of most other realizable circuit topologies, they were chosen as benchmark cases for the analysis. Most other likely chosen topologies for microgrids, including, but not limited to buck–boost, flyback, Ćuk, push–pull, or half-bridge, have similar number of components and arrangement than one of the
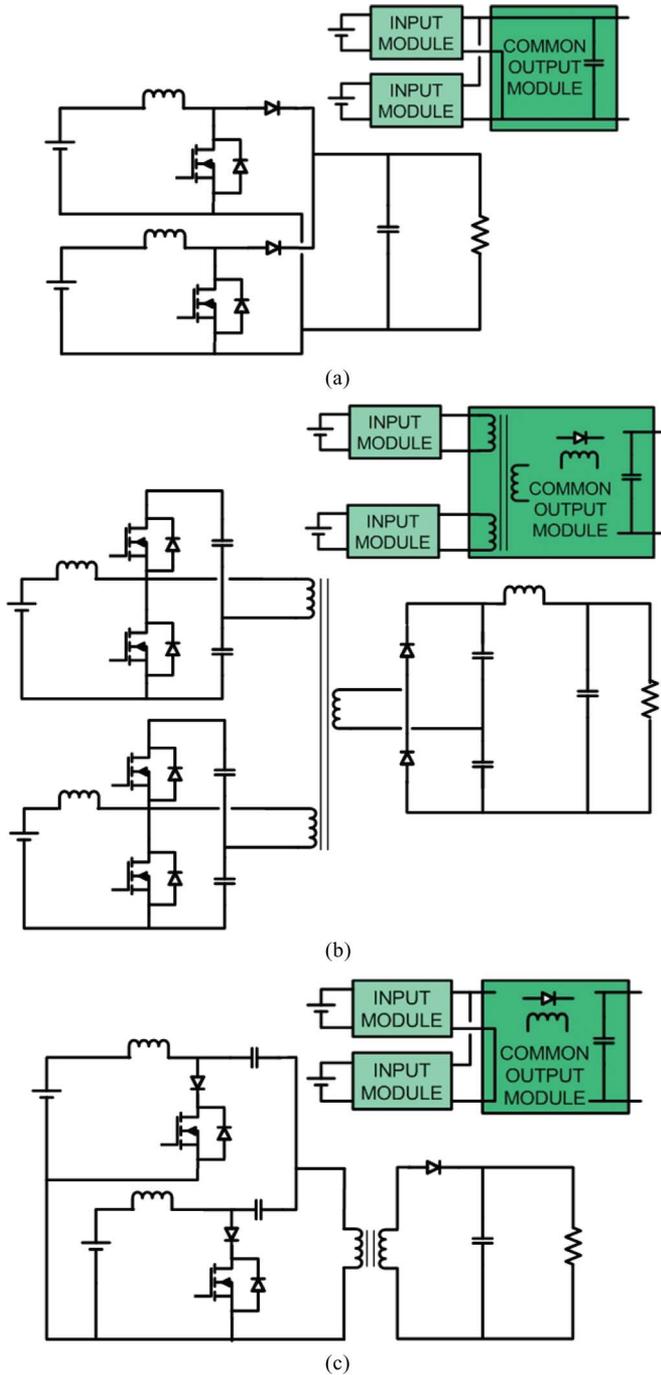
(a)

(b)

(c)

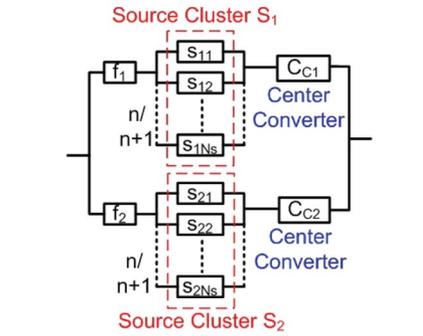Fig. 3. Three possible MICs topologies. (a) Boost. (b) CSHB [40]. (c) ISEPIC.
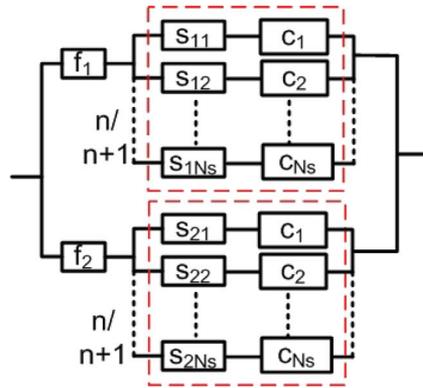

Fig. 4. Microgrid Configuration A.

Fig. 5. Microgrid Configuration B.

with discontinuous currents, current source interface converters facilitates maximum power point tracking (MPPT) and almost eliminate current ripple that may reduce MPPT algorithms efficacy. Moreover, contrary to the boost converter, the ISEPIC can be controlled to both increase and decrease the DG unit voltage, so the entire output characteristic of the source can be tracked in search for a maximum power point of operation [43]. Furthermore, the ISEPIC and CSHB may have high-voltage step-up conversion ratios, so sources with inherently low voltages, such as photovoltaic (PV) modules and fuel cells, can be easily integrated without compromising reliability by connecting many power generation cells in series [44], [45].

C. Assumptions and Additional Considerations

Figs. 4–9 show a diagram of six of the more general dc microgrid architectures. In these figures, f represents the fuel supply for the DG sources, s is each DG source unit, C_C is a center converter, c is a SIC converter module, i represents a MIC input module, and o is a MIC common output stage module. The last two of the six architectures include MICs. The analysis assumes that two different types of DG sources are used and that the microgrid counts with more than one unit for each DG source technology. These DG units are grouped in two clusters, with each cluster having all DG sources of the same technology. In order to be able to compare all configurations, it is assumed unless clarified otherwise that each source cluster and each converter arrangement have an $n + 1$ redundant configuration. Hence, in all cases, at least n operating DG units and converters are needed

three reference circuits, so difference in reliability calculations with the corresponding similar topology of these other converters are negligible. The three chosen topologies have some subtle differences that make them, from a practical perspective, slightly more likely to be chosen for microgrid interfaces. All three, boost, ISEPIC, and CSHB converters, have a current source interface, which makes them suitable to all type of sources, particularly to those, such as fuel cells, that require relatively continuous current output. In addition to provide "universal" source compatibility and avoid affecting fuel cells life
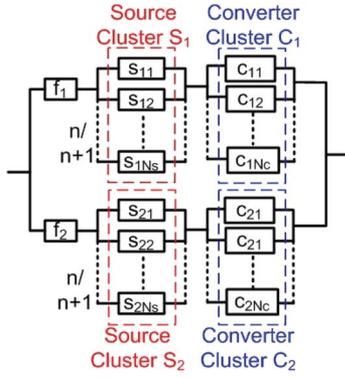
Fig. 6.   Microgrid Configuration C.

to power the load. Evidently, DG sources and converter modules can be selected for a relatively higher rated power, but such a condition will lead to a better availability than that obtained with the previous assumption because the microgrid can absorb failures in more DG units or converter modules without leading to overall system failure. For the cases with MICs, it is assumed that each MIC has two input modules, each connected to a different source type, and that the output stage is rated at double the power than that of the input stages. That is, each output stage is able to carry the load of both of its input stages operating simultaneously at their respective rated power. In order to compare all circuit topologies on equal basis, it is also assumed that converters circuit components are selected so that each of them are equally stressed in all three circuit topologies and all six configurations. In case some insights on the relative reliability difference among circuit topologies based on components potential stress levels are desired, the reader can resort to [26] for such information. It is also assumed that all configurations have distributed and autonomous controllers, such as the one in [29], so availability is not negatively affected by communication links or centralized controllers, such as the one considered in [46], which can act as single point of failures.

The six studied architectures are as follows:

1) *Configuration A (see Fig. 4):* A center SIC for each source cluster.
2) *Configuration B (see Fig. 5):* One SIC for each DG unit.
3) *Configuration C (see Fig. 6):* Nonredundant or $n + 1$ redundant arrangement of SICs for each DG cluster.
4) *Configuration D (see Fig. 7):* Nonredundant or $n + 1$ redundant arrangement of SICs for each DG unit.
5) *Configuration E (see Fig. 8):* Nonredundant or $n + 1$ redundant arrangement of MICs with each source of the same type connected in parallel to form a cluster. Each of the two input modules of a MIC module is connected to a different source cluster. Its SIC counterpart is Configuration C.
6) *Configuration F (see Fig. 9):* One MIC input module connected to each DG unit. Its SIC counterpart is Configuration B.

Examples of microgrids operational behavior with some relevant configurations are shown in Figs. 10–12. These figures
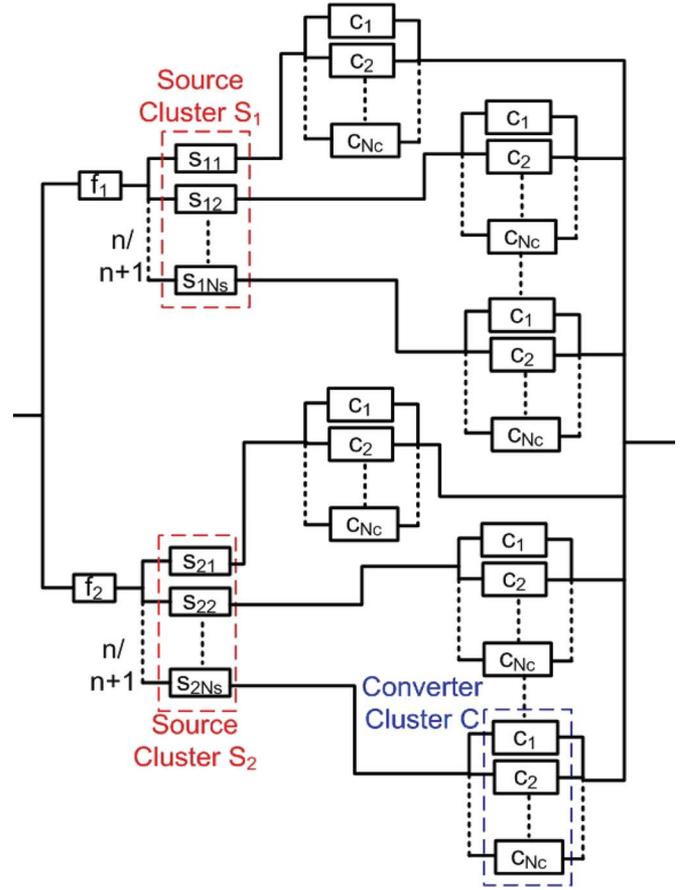

Fig. 7.   Microgrid Configuration D.
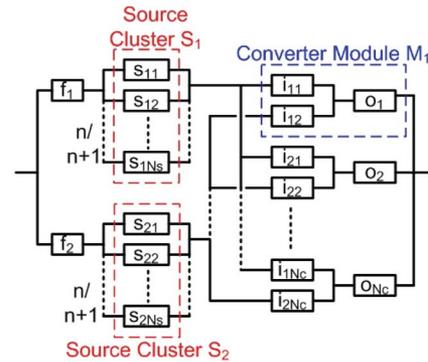

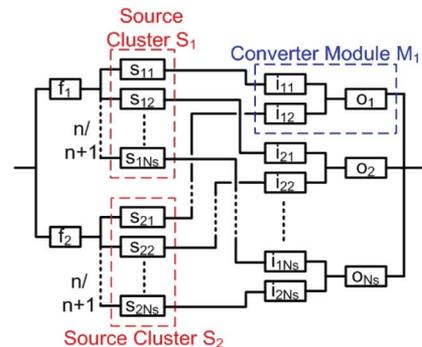Fig. 8.   Microgrid Configuration E.

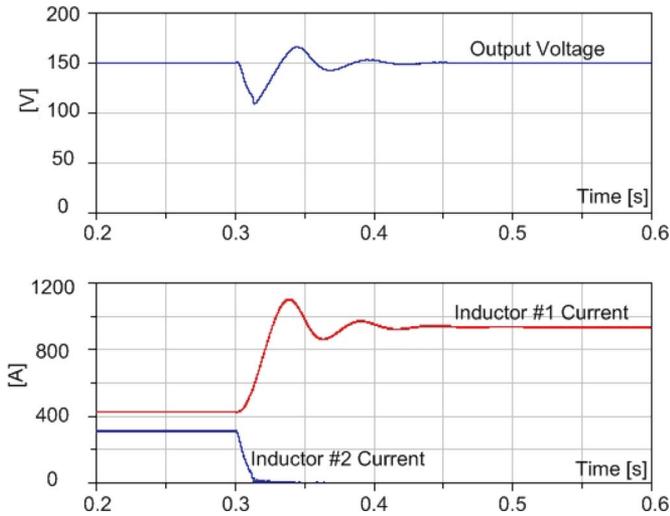
Fig. 9.   Microgrid Configuration F.

Fig. 10.   Simulation showing the behavior of Configuration A with CSHB when a failure occurs at $t = 0.3$ s.
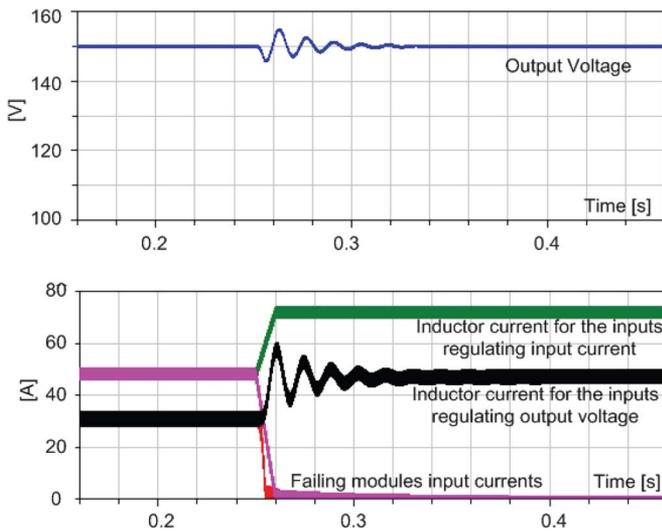

Fig. 11.   Simulation showing the behavior of Configuration C with boost converters when failures occur at $t = 0.25$ s.
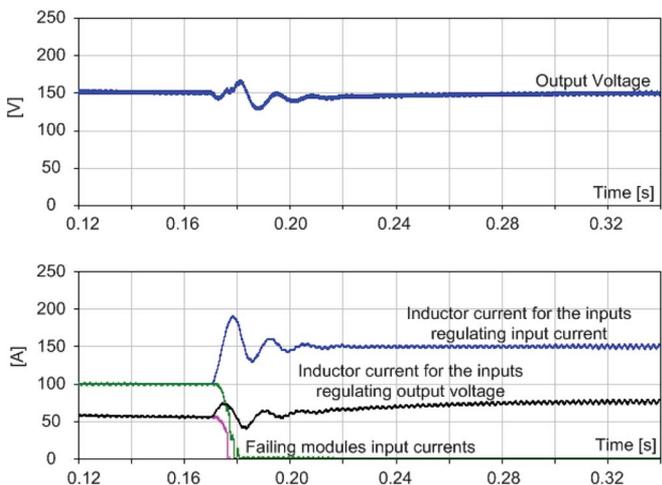

Fig. 12.   Simulation showing the behavior of Configuration F with MI ISEPICs when failures occur at $t = 0.17$ s.

display simulation results for some key scenarios with different architecture configurations and circuit topologies. In all these cases, one converter cluster or one set of input legs corresponding to the same source type control output voltage, while the remaining converter cluster or input legs share a same portion of a total input current target. All converter modules are $n + 1$ redundant. Fig. 10 shows a simulated case of Configuration A with CSHB converters with one source cluster producing 48 V and the other 36 V. Both input inductors have 300 μH inductances, output capacitances equal 1000 μF, and all other capacitances are 100 μF. The output voltage is regulated to 150 V through the high-voltage source path with an integral controller with a gain of 0.2. The other power path regulates the output current of the source to 312 A with an integral controller with a gain of 0.1. This current regulating converter fails at $t = 0.3$ s. Fig. 11 shows the case of Configuration C with three boost converters in each converter cluster. The voltage produced by the sources are 48 and 36 V. The output voltage is regulated by the converters connected to the high-voltage sources to 150 V with an integral controller with a gain of 0.25. Input currents for the converters connected to the low-voltage source are regulated to a total of 144 A, which is initially divided equally into 48 A for each of these three converters. Current regulators are PI controllers with an integral gain of 0.1 and a proportional gain of 10. These boost converters have 300 μH inductors and 500 μF capacitors. A failure in one of the high-input voltage boost converters and in one of the low-input voltage converters occurs at $t = 0.25$ s. The last example is shown in Fig. 12. In this figure, Configuration F was simulated with three MI ISEPIC modules, each with two input legs. The sources output are 48 and 24 V. The input inductors for the ISEPIC have an inductance of 500 μH. The center capacitors have a capacitance of 100 μF and the output capacitors have a capacitance of 300 μF. Output voltage is regulated to 150 V by the high-input voltage legs with an integral controller with a gain of 0.25. The other input legs regulate input current with an integral controller with a gain of 0.5. Their total current target is 300 A, initially divided equally in 100 A for each leg until a failure affects one input leg of each source cluster. In all cases, the load is a 2 Ω resistance, which is kept powered despite the failure in the source interfaces due to adequate $n + 1$ redundant design—in these examples, all $n + 1$ redundant modules are designed and operated so if one of them fails, the others can still absorb its load.

In addition to the aforementioned assumptions, it is being considered that all sources are dispatchable and that their source of energy is a continuous flow of fuel with a given availability. The reason for considering dispatchable sources fueled with a continuous flow is to avoid distracting the analysis, which is focused on the power electronic interfaces and system architecture, with issues and peculiarities affecting the DG sources. Although issues and particularities affecting sources are out of the scope of this paper, an explanation on how to consider discontinuous fuel flow through local storage is provided in a later section of this paper. For the case of renewable sources that are not typically dispatchable, such as PV generators, it is assumed that they are collocated with enough energy storage, so the source availability is equivalent to that of dispatchable

sources. In case it is desired, the quantitative approach presented in this paper may also serve to calculate a microgrid's availability when using nondispatchable sources. Previous works, such as [47], may assist in this calculation by relating PV generation availability with energy storage sizing and solar energy generating profile. For the same reason that it is being considered that all sources are dispatchable and they receive a continuous fuel supply, it is also being assumed that all sources in the dc microgrid operate in hot standby and that no energy storage needs to be added to the microgrid in order to increase its availability. These assumptions represent typical operation and engineering approaches in microgrids [8] and also present a paradigm shift in ultra available systems with respect to conventional energy systems that achieve high availability by combining cold standby diesel generators with local energy storage in batteries. Comparison between these two paradigms—microgrids with local power generation versus local conventional energy systems with energy storage and standby generators—will be performed also in a later section of this paper.

III. MCS-BASED AVAILABILITY ANALYSIS

The availability of the configurations under study cannot be studied by completely reducing their availability success diagram in steps by taking advantage of series and parallel arrangements of components because of two reasons. One of these two reasons is that some configurations, such as those with MICs, have meshed structures that are neither a series nor a parallel arrangement. The other reason is that adequate operation of the microgrid—i.e., the load can be fully powered—requires just that a given number of sources N_{Sm} are operational from the total pool of source units from both clusters, each with N_S sources. With $n + 1$ redundancy N_{Sm} equals $N_S - 1$, whereas without redundancy N_{Sm} equals N_S. Hence, successful operation of the sources cannot be represented in an availability success diagram by a parallel combination of sources in each cluster, either with or without redundancy. Markov availability analysis is also inadequate because of the large number of states involved. Instead, the method proposed here calculates availability by identifying all mcs—the sets of components such that if all of them fail, the system also fails, but that if any one of the elements of the list is removed from the set, then the system is no longer failed—and then consider that the microgrid unavailability U_{MG} equals

$$U_{MG} = P\left(\bigcup_{j=1}^{M_C} K_j\right) \quad (2)$$

where K_j represents the mcs, $P(K_j)$ is the mcs probability, and M_C is the total number of mcs. Calculation of (2) is usually extremely tedious. However, the calculation can be simplified by recognizing that U_{MG} is bounded by [35]

$$\sum_{i=1}^{M_c} P(K_i) - \sum_{i=2}^{M_c}\sum_{j=1}^{i-1} P(K_i \cap K_j) \leq U_{MG} \leq \sum_{i=1}^{M_c} P(K_i) \quad (3)$$

TABLE I
MCS DESCRIPTION, PROBABILITY, AND QUANTITY FOR CONFIGURATION A

mcs #	Minimal cut sets	Quantity and probability of occurrence	$n+1$ Redundancy
1	$\{f_1, f_2\}$	$(1)(u_{f1}u_{f2})$	N/A
2	$\{Cc_1, Cc_2\}$	$(1)(u_{CC}u_{CC})$	N/A
3	$\{f_2, Cc_1\},\{f_1, Cc_2\}$	$u_{f1}u_{CC} + u_{f2}u_{CC}$	N/A
4_{NR}	$\{f_1,s_{2k}\}, \{f_2, s_{1k}\}$	$N_S(u_{S2}u_{f1} + u_{S1}u_{f2})$	Sources: No
4_R	$\{f_1, s_{2m}, s_{2k}\}, \{f_2, s_{1m}, s_{1k}\}.$	$C_2^{N_S}(u_{S1}^2 u_{f2} + u_{S2}^2 u_{f1})$	Sources: Yes
5_{NR}	$\{C_{C1},s_{2k}\}, \{C_{C2}, s_{1k}\}$	$N_S(u_{S2} + u_{S1})u_{CC}$	Sources: No
5_R	$\{i_{1k}, i_{1l}, i_{2m}, i_{2n}\}$	$C_2^{N_S}(u_{S1}^2 + u_{S2}^2)u_{CC}$	Sources: Yes
6_{NR}	One fewer operating source unit than the minimum required.	$\sum_{j=1}^{N_S} C_j^{N_S} C_{N_S-j+1}^{N_S} u_{S1}^j u_{S2}^{N_S-j+1}$	Sources: No
6_R	One fewer operating source unit than the minimum required.	$\sum_{j=2}^{N_S} C_j^{N_S} C_{N_S-j+2}^{N_S} u_{S1}^j u_{S2}^{N_S-j+2}$	Sources: Yes

TABLE II
MCS DESCRIPTION, PROBABILITY, AND QUANTITY FOR CONFIGURATION B

mcs #	Minimal cut sets	Quantity and probability of occurrence	$n+1$ Redundancy
1	$\{f_1, f_2\}$	$(1)(u_{f1}u_{f2})$	N/A
2_{NR}	$\{f_1, (s_{2k},c_{2k})\},$ $\{f_2, (s_{1k},c_{1k})\}$	$N_S(u_{SC2}u_{f1} + u_{SC1}u_{f2})$	Sources: No
2_R	$\{f_1, (s_{2k},c_{2k}), (s_{2m},c_{2m})\},$ $\{f_2, (s_{1k},c_{1k}), (s_{1m},c_{1m})\}$	$C_2^{N_S}(u_{SC1}^2 u_{f2} + u_{SC2}^2 u_{f1})$	Sources: Yes
3_{NR}	One fewer operating pair DG unit-SIC than the minimum required.	$\sum_{j=1}^{N_S} C_j^{N_S} C_{N_S-j+1}^{N_S} u_{SC1}^j u_{SC2}^{N_S-j+1}$	Sources: No
3_R	One fewer operating pair DG unit-SIC than the minimum required.	$\sum_{j=2}^{N_S} C_j^{N_S} C_{N_S-j+2}^{N_S} u_{SC1}^j u_{SC2}^{N_S-j+2}$	Sources: Yes

because with highly available components, as it occurs here, U_{MG} can be very accurately approximated to

$$U_{MG} \cong \sum_{j=1}^{M_C} P(K_j). \quad (4)$$

Tables I–VI indicate the mcs description—second column—and their corresponding contributing term in (4)—third column—for configurations A to F, respectively. The fourth column in those tables indicates whether or not the mcs probability of the respective row needs to be considered, depending on the redundancy policy. The redundancy policy refers only to components contained in the respective mcs. All missing failure conditions do not present mcs. Nomenclature used in these tables is specified in Appendix A. In order to exemplify how these tables are formed, consider Table IV. In this table, mcs #1 represents the failure of both fuel supplies. Also in Table IV, the mcs #2_{NR} represents the case in which, with no redundancy in the source clusters, one of the fuel supplies fails and one of the pairs formed by a DG unit fueled by the other fuel supply and its corresponding cluster of SICs fails. Mcs 2_R represent the same failure mode, but when there is an $n + 1$ redundant arrangement of sources. In both mcs #2_{NR} and #2_R, the SIC clusters can be considered with or without redundant configurations. If the SIC arrangement is redundant, then (25)—indicated in the Appendix A —is used in the calculations. Otherwise (24) should be used.

TABLE III
MCS DESCRIPTION, PROBABILITY, AND QUANTITY FOR CONFIGURATION C

mcs #	Minimal cut sets	Quantity and probability of occurrence	$n+1$ Redundancy
1	$\{f_1, f_2\}$	$(1)(u_{f1}u_{f2})$	N/A
2_{NR}	$\{f_2, s_{1k}\}$ and $\{f_1, s_{2k}\}$	$N_S(u_{s1}u_{f2}) + N_S(u_{s2}u_{f1})$	No
2_R	$\{f_2, s_{1m}, s_{1k}\}$ and $\{f_1, s_{2m}, s_{2k}\}$	$C_2^{N_S}(u_{f1}u_{s2}^2) + C_2^{N_S}(u_{f2}u_{s1}^2)$	Yes
3_{NR}	One fewer operating DG unit than the minimum required for the system to operate.	$\sum_{j=1}^{N_s} C_j^{N_S} C_j^{N_S-j+1} u_{s1}^{N_S+1-j} u_{s2}^j$	No
3_R	One fewer operating DG unit than the minimum required for the system to operate.	$\sum_{j=1}^{N_s} C_j^{N_S} C_j^{N_S-j+2} u_{s1}^{N_S+2-j} u_{s2}^j$	Yes
4_{NR}	$\{c_{1k}, c_{2m}\}$	$N_C u_C^2$	No
4_R	$\{c_{1k}, c_{1p}, c_{2m}, c_{2n}\}$	$C_2^{N_C} u_C^4$	Yes
7_{NR}	$\{f_1, c_{2k}\}, \{f_2, c_{1k}\}$	$N_C(u_{f1}+u_{f2})u_C$	No
7_R	$\{f_1,c_{2k}, c_{2p}\}, \{f_2, c_{1k}, c_{1p}\}$	$C_2^{N_C}(u_{f1}+u_{f2})u_C^2$	Yes
8_{NR}	$\{\{S_1\},c_{2k}\}, \{\{S_2\}, c_{1k}\}$	$N_C(u_{s1}^{N_S} + u_{s2}^{N_S})u_C$	No: input NR: sources
8_R	$\{\{S_1\},c_{2k}, c_{2p}\}, \{\{S_2\}, c_{1k}, c_{1p}\}$	$C_2^{N_C}(u_{s1}^{N_S} + u_{s2}^{N_S})u_C^2$	Yes: input NR: sources
9	One fewer operating DG unit and one fewer operating SIC than the minimum required for the system to operate.	$\sum_{j,k \in \Psi} C_{N_S-j}^{N_S} C_{N_C-k}^{N_C}(u_{s1}^{N_S-j} + u_{s2}^{N_S-j})u_C^{N_C-k}$ **	NR

$$**\Psi = \left\{1 \le j \le N_S, 1 \le k \le N_C : \frac{j}{n_s} + \frac{k}{n_c} < 1 \circ \frac{j}{n_s} + \frac{k}{n_c} + \frac{1}{n_c} \ge 1 \circ \frac{j}{n_s} + \frac{k}{n_c} + \frac{1}{n_s} \ge 1\right\}.$$

TABLE IV
MCS DESCRIPTION, PROBABILITY, AND QUANTITY FOR CONFIGURATION D

mcs #	Minimal cut sets	Quantity and probability of occurrence	$n+1$ Redundancy
1	$\{f_1, f_2\}$	$(1)(u_{f1}u_{f2})$	N/A
2_{NR}	$\{f_1, (s_{2k},C_{2k})\}$, $\{f_2, (s_{1k}, C_{1k})\}$	$N_S(u_{Sb2}u_{f1}+ u_{Sb1}u_{f2})$	Sources: No SICs: *
2_R	$\{f_1, (s_{2k},C_{2k}), (s_{2m},C_{2m})\}$, $\{f_2, (s_{1k}, C_{1k}), (s_{1m},C_{1m})\}$	$C_2^{N_s}(u_{Sb1}^2 u_{f2} + u_{Sb2}^2 u_{f1})$	Sources: Yes SICs: *
3_{NR}	One fewer operating pair DG unit-SIC group than the minimum required.	$\sum_{j=1}^{N_s} C_j^{N_S} C_{N_S-j+1}^{N_S} u_{Sb1}^j u_{Sb2}^{N_S-j+1}$	Sources: No SICs: *
3_R	One fewer operating pair DG unit-SIC group than the minimum required.	$\sum_{j=2}^{N_s} C_j^{N_S} C_{N_S-j+2}^{N_S} u_{Sb1}^j u_{Sb2}^{N_S-j+2}$	Sources: Yes SICs: *

* See note about calculation of u_{Sbk} and A_C in Appendix A.

Mcs #3_R and #3_{NR} are a group of mcs that exemplify why simpler approaches, such as availability success diagram reduction, cannot be applied in this study. These mcs represent a condition in which there is just one fewer source among all the DG units in both clusters than the minimum needed to fully power the load. Hence, each mcs #3_{NR} includes $N_S + 1$ failed DG units from the total of twice N_S source units contained in both clusters. Similarly, each mcs #3_R includes $N_S + 2$ failed DG units from the total of twice N_S source units contained in both clusters. Hence, when sources have redundant arrangements, the unavailability for Configuration D is as follows:

$$U_{MG} = u_{f1}u_{f2} + C_2^{N_S}\left(u_{Sb1}^2 u_{f2} + u_{Sb2}^2 u_{f1}\right)$$
$$+ \sum_{j=2}^{N_S} C_j^{N_S} C_{N_S-j+2}^{N_S} u_{Sb1}^j u_{Sb2}^{N_S-j+2}. \quad (5)$$

When their sources are not arranged in clusters with redundant sources, the unavailability for Configuration D is as follows:

$$U_{MG} = u_{f1}u_{f2} + N_S\left(u_{Sb2}u_{f1} + u_{Sb1}u_{f2}\right)$$
$$+ \sum_{j=1}^{N_S} C_j^{N_S} C_{N_S-j+1}^{N_S} u_{Sb1}^j u_{Sb2}^{N_S-j+1}. \quad (6)$$

Mcs #9 in Tables III and V and #13 in Table V require some additional explanation. In order to understand the reasoning behind these mcs, consider mcs #9 in Table V. This mcs consider cases in which although the total number of DG units and inputs modules would be sufficient to power the load, it is not fully powered because of how working DG units and input modules are distributed in the microgrid architecture. For example, consider that there is no redundancy and there are five DG units in each source cluster. Hence, if the load has a power of P_L watts, each DG unit is rated at $P_L N_S/5$ watts and at least N_S source units are required to power the load. Now consider that there are ten converter modules. Each input module is rated at $P_L N_C/10$ and at least N_C working modules are needed to power the load. Now consider that source cluster #1 has two working units and source cluster #2 has all its DG units working. Also consider that there are four operating input modules connected to the source cluster #2 and that all input modules connected to the source cluster #1 are working. Since the total working DG units is more than N_S and the total operating input modules is more than N_C, it may seem that the system is able to power the load. However, since the load can only receive $2P_L N_S/5$ watts from the source cluster #1—40% of P_L—and $4P_L N_C/10$ watts from source cluster #2—another 40% of P_L—then the microgrid is unable to fully power the load. Hence, it is failed. Still, in this

TABLE V
Mcs Description, Probability, and Quantity for Configuration E

mcs #	Minimal cut sets	Quantity and probability of occurrence	$n+1$ Redundancy
1	$\{f_1, f_2\}$	$(1)(u_{f1}u_{f2})$	N/A
2$_{NR}$	$\{f_2, s_{1k}\}$ and $\{f_1, s_{2k}\}$	$N_S(u_{S1}u_{f2}) + N_S(u_{S2}u_{f1})$	No
2$_R$	$\{f_2, s_{1m}, s_{1k}\}$ and $\{f_1, s_{2m}, s_{2k}\}$	$C_2^{N_s}(u_{f1}u_{s2}^2) + C_2^{N_s}(u_{f2}u_{S1}^2)$	Yes
3$_{NR}$	One fewer operating DG unit than the minimum required for the system to operate.	$\sum_{j=1}^{N_s} C_j^{N_s} C_j^{N_s-j+1} u_{s1}^{N_s+1-j} u_{s2}^j$	No
3$_R$	One fewer operating DG unit than the minimum required for the system to operate.	$\sum_{j=1}^{N_s} C_j^{N_s} C_j^{N_s-j+2} u_{s1}^{N_s+2-j} u_{s2}^j$	Yes
4$_{NR}$	$\{i_{1k}, i_{2m}\}$	$N_C u_i^2$	No
4$_R$	$\{i_{1k}, i_{1p}, i_{2m}, i_{2n}\}$	$C_2^{N_c} u_i^4$	Yes
5$_{NR}$	$\{o_k\}$	$N_C u_o$	No
6$_R$	$\{o_k, o_p\}$	$C_2^{N_c} u_o^2$	Yes
7$_{NR}$	$\{f_1, i_{2k}\}, \{f_2, i_{1k}\}$	$N_C(u_{f1}+u_{f2})u_i$	No
7$_R$	$\{f_1, i_{2k}, i_{2p}\}, \{f_2, i_{1k}, i_{1p}\}$	$C_2^{N_c}(u_{f1}+u_{f2})u_i^2$	Yes
8$_{NR}$	$\{\{S_1\}, i_{2k}\}, \{\{S_2\}, i_{1k}\}$	$N_C(u_{s1}^{N_s}+u_{s2}^{N_s})u_i$	No: input NR: sources
8$_R$	$\{\{S_1\}, i_{2k}, i_{2p}\}, \{\{S_2\}, i_{1k}, i_{1p}\}$	$C_2^{N_c}(u_{s1}^{N_s}+u_{s2}^{N_s})u_i^2$	Yes: input NR: sources
9	One fewer operating DG unit and one fewer operating input leg than the minimum required for the system to operate	$\sum_{j,k\in\Psi} C_{N_s-j}^{N_s} C_{N_c-k}^{N_c}(u_{s1}^{N_s-j}+u_{s2}^{N_s-j})u_i^{N_c-k}$ **	NR
10	$\{i_{1k}, o_p\}, \{i_{2k}, o_p\}$	$N_C(N_C-1)^2 u_i^2 u_o$	Yes
11	$\{f_1, i_{2k}, o_p\}, \{f_2, i_{1k}, o_p\}$	$N_C(N_C-1)(u_{f1}+u_{f2})u_i u_o$	Yes
12	$\{\{S_1\}, i_{2k}, o_p\}, \{\{S_2\}, i_{1k}, o_p\}$	$N_C(N_C-1)(u_{s1}^{N_s}+u_{s2}^{N_s})u_i u_o$	Yes: converters NR: sources
13	One fewer operating DG unit and one fewer operating input leg and one fewer operating output stage than the minimum required for the system to operate	$N_C \sum_{j,k\in\Psi} C_{N_s-j}^{N_s} C_{N_c-k}^{N_c-1}(u_{s1}^{N_s-j}+u_{s2}^{N_s-j})u_i^{N_c-k} u_o$ **	Yes: converters NR: sources

$$**\Psi = \left\{ 1\le j \le N_S, 1 \le k \le N_C : \frac{j}{n_s}+\frac{k}{n_C} < 1 \circ \frac{j}{n_s}+\frac{k}{n_C}+\frac{1}{n_C} \ge 1 \circ \frac{j}{n_s}+\frac{k}{n_C}+\frac{1}{n_s} \ge 1 \right\}.$$

past example, the set of all failed input modules #2 and all failed DG units #1 does not constitutes a mcs because if one of the input modules is repaired, the system will still be in a failed condition. Therefore, four conditions need to be satisfied in order to have an mcs associated to the aforementioned operational state. The first condition is that all failed input modules are connected to a source cluster with all working units; whereas the output of the source cluster with failed units are powering a cluster of operational input modules. The second condition states that the system is in its failed state. That is, the number of working DG units N_{WS} in the source cluster with failures and the number of operational input modules N_{Wi} among the failed cluster of input modules satisfies

$$\frac{N_{WS}}{N_S} + \frac{N_{Wi}}{N_C} < 1. \tag{7}$$

The third and four conditions represent the condition to have mcs, i.e., if one DG unit is repaired with respect to (7), the system can power the load again

$$\frac{N_{WS}}{N_S} + \frac{N_{Wi}}{N_C} + \frac{1}{N_S} \ge 1 \tag{8}$$

and if one input module is repaired with respect to (7), the system can power the load again

$$\frac{N_{WS}}{N_S} + \frac{N_{Wi}}{N_C} + \frac{1}{N_C} \ge 1. \tag{9}$$

All (7)–(9) become explicit if both sides are multiplied by P_L. When the redundancy policy is considered, conditions (7)–(9) create the set Ψ of pairs (j,k) indicated in Tables III and V.

IV. DISCUSSION

A. Effects of Converter Topology and System Architecture on Microgrid Availability

In order to evaluate in a quantitative way, each of the microgrid architecture and circuit topologies benchmarking cases consider the typical component reliability values in Table VII. Since grid availability is higher than that of any DG unit, it is assumed that the analysis is made either for a stand-alone microgrid or for a microgrid operation when the grid is out of service. The results will, then, provide a worst case scenario view, which can only be better if a main power grid is providing power to the microgrid. This assumption also facilitates the analysis of

TABLE VI
MCS DESCRIPTION, PROBABILITY, AND QUANTITY FOR CONFIGURATION F

mcs #	Minimal cut sets	Quantity and probability of occurrence	$n+1$ Redundancy
1	$\{f_1, f_2\}$	$(1)(u_{f1}u_{f2})$	N/A
2_{NR}	$\{f_2, s_{1k}\}$ and $\{f_1, s_{2k}\}$	$N_S(u_{S1}u_{f2}) + N_S(u_{S2}u_{f1})$	No
2_R	$\{f_2, s_{1m}, s_{1k}\}$ and $\{f_1, s_{2m}, s_{2k}\}$	$C_2^{N_S}(u_{f1}u_{S2}^2) + C_2^{N_S}(u_{f2}u_{S1}^2)$	Yes
3_{NR}	One fewer operating pair DG unit-MIC input module than the minimum required for the system to operate.	$\sum_{j=1}^{N_s} C_j^{N_S} C_j^{N_S-j+1} u_{si1}^{N_S+1-j} u_{si2}^{j}$	No
3_R	One fewer operating pair DG unit-MIC input module than the minimum required for the system to operate.	$\sum_{j=1}^{N_s} C_j^{N_S} C_j^{N_S-j+2} u_{si1}^{N_S+2-j} u_{si2}^{j}$	Yes
5_{NR}	$\{o_k\}$	$N_C u_o$	No
6_R	$\{o_k, o_p\}$	$C_2^{N_S} u_o^2$	Yes
7_{NR}	$\{f_1, i_{2k}\}, \{f_2, i_{1k}\}$	$N_S(u_{f1}+u_{f2})u_i$	No
7_R	$\{f_1, i_{2k}, i_{2p}\}, \{f_2, i_{1k}, i_{1p}\}$	$C_2^{N_S}(u_{f1}+u_{f2})u_i^2$	Yes
8_{NR}	$\{\{S_1\}, i_{2k}\}, \{\{S_2\}, i_{1k}\}$	$N_S(u_{s1}^{N_S}+u_{s2}^{N_S})u_i$	No
8_R	$\{\{S_1\}, i_{2k}, i_{2p}\}, \{\{S_2\}, i_{1k}, i_{1p}\}$	$C_2^{N_S}(u_{s1}^{N_S}+u_{s2}^{N_S})u_i^2$	Yes
9	$\{f_1, (s_{2k}i_{2k}), o_p\}, \{f_2, (s_{1k}i_{1k}), o_p\}$	$N_S(N_S-1)(u_{f1}u_{Si2} + u_{f2}u_{Si1})u_o$	Yes
10	$\{\{S_1\}, (s_{2k}i_{2k}), o_p\}, \{\{S_2\}, (s_{1k}i_{1k}), o_p\}$	$N_S(N_S-1)(N_S-2)(u_{si1}^{N_S-1}+u_{si2}^{N_S-1})u_i u_o$	Yes
11	$\{(s_{2k}i_{2k}), (s_{1k}i_{1k}), o_p\}, \{(s_{1k}i_{2k}), (s_1 i_{1k}), o_p\}$	$N_S u_o \sum_{j=1}^{N_s-1} C_j^{N_S-1} C_{N_S-j}^{N_S-1} u_{si1}^{j} u_{si2}^{N_S-j}$	Yes

the conditions necessary for a microgrid to achieve ultrahigh availability. Table VII also contains the calculated failure and repair rates for the MIC and SIC topologies used as benchmarks. It is assumed that the maintenance policy indicates that no spare converter modules are kept at the microgrid site, so it takes about a week to replace any damaged unit. The results of the availability calculations that consider $n + 1$ redundancy for both converter modules and DG units are summarized numerically in Table VIII and graphically in Fig. 13. In this figure, the vertical axis absolute value is also approximately equal to the microgrid availability measured in "nines." It was assumed that sources for cluster #1 are microturbines and for cluster #2 are fuel cells. In order to equalize the comparison of configurations in which the number of sources equal the number of converter (input) modules—B and F—with those in which n_S can be chosen different from n_C—C, D, and E—it was also assumed that both n_S and n_C equal 5. Still, calculations indicate that provided $n + 1$ redundancy is maintained and n_C is reasonably low (e.g., below 15), varying values for n_C yields marginal differences in the availability of configurations C, D, or E. In order to simplify the analysis and to avoid affecting the study focus on the converters by considering the effect of local energy storage in the fuel supply, u_{F1} was consider equal to u_{F2}. The table and figure indicate that except for Configuration A with an availability below 6-nines, all other cases are approximately equal in terms of availability, with a value of about 6.5-nines. Yet, configurations E and F require fewer components than their SIC configuration counterparts and, hence, microgrid architectures with MICs have potential for cost savings without compromising availability as it occurs with conventional approaches [55]. Evidently, Case A is the worst in terms of availability, but it is the one that utilizes fewer components. The opposing case by a

TABLE VII
RELIABILITY VALUES USED IN THE NUMERICAL EXAMPLES ([48] BASED ON [49] UNLESS SPECIFIED OTHERWISE)

Item and origin of the value	MTTF or MUT (hours)	MDT (hours)	Availability a
MOSFET (temperature adjusted)	12.5 M	Non repairable	
Diode (temperature adjusted)	41.6 M	Non repairable	
Electrolytic capacitor	16.6 M	Non repairable	
Winding	25 M	Non repairable	
Control stage	3.3 M	Non repairable	
Film Capacitor	20 M	Non repairable	
Fuel Cell (performance degradation) [50]	5000	166.6	0.967742
Microturbine [4]	8000	50	0.993789
Center SIC or SIC module	1 M	166.6	0.999833
Input module for Boost MIC	2.25 M	166.6	0.999926
Output module for Boost MIC	16.6 M	166.6	0.999990
Input module for ISEPIC MIC	1.93 M	166.6	0.999914
Output module for ISEPIC MIC	6.1 M	166.6	0.999972
Input module for CSHB MIC	1.51 M	166.6	0.999897
Output module for CSHB MIC	2.72 M	166.6	0.999938
Typical telecom rectifier [6]	0.5 M	166.6	0.999667
Diesel generator (Average from [4], [51] − [54]) (ρ_{GS}=0.0241) [4]	823	5	0.9939
U.S.electric grid [4]	2440	2.08	0.999150
Bio fuel for microturbine / Natural gas for fuel cell with reformer [4]	2 M	50	0.999975

marginal difference in terms of availability is Configuration D. Still, it is extremely inefficient in terms of part counts, requiring by far the most number of components of all cases.

The previous calculations show that use of MIC reduces the common need of trading off availability for part counts and, hence, potentially costs in power electronic interfaces. Still, since DG units typically contribute to a significant portion of

TABLE VIII
SYSTEM AVAILABILITY FOR THE STUDIED CASES

| Case	SIC or MIC Topology	U_{MG} (10^{-7})	Availability
A	Boost	17.76	0.99999822381
A	ISEPIC	22.64	0.99999773634
A	CSHB	31.06	0.99999689427
B	Boost	4.08	0.99999959234
B	ISEPIC	4.08	0.99999959150
B	CSHB	4.10	0.99999959006
C	Boost	4.05	0.99999959469
C	ISEPIC	4.05	0.99999959468
C	CSHB	4.05	0.99999959468
D	Boost	4.05	0.99999959469
D	ISEPIC	4.05	0.99999959468
D	CSHB	4.05	0.99999959466
E	Boost	4.07	0.99999959318
E	ISEPIC	4.17	0.99999958345
E	CSHB	4.62	0.99999953815
F	Boost	4.07	0.99999959290
F	ISEPIC	4.17	0.99999958269
F	CSHB	4.64	0.99999953649
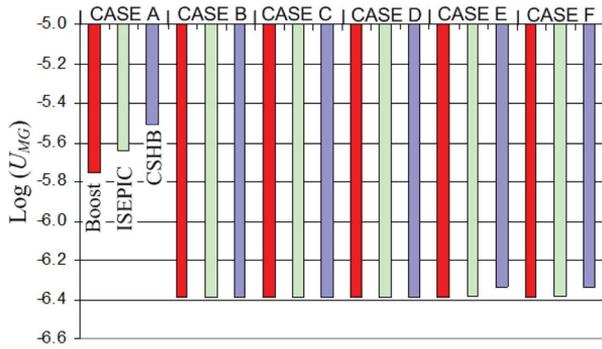
Fig. 13. Summary of unavailabilities from Table VIII for the six studied cases and three benchmark topologies.

the cost, it is relevant to evaluate how availability is impacted if no redundancy is used in the source clusters (but it is still used for converters for those cases in which the number of converters can be different from that of the source). With no source redundancy and considering an ISEPIC as the converter topology, all cases have approximately the same unavailability of 4.82×10^{-6}—meaning an availability of about 5.5 nines—except for Configuration A with an unavailability of 2.7×10^{-5}. Without redundancy in the sources, availability for configurations B through F is still very high due to the use of diverse power sources. Without source diversity, availability drops sharply because if only one cluster of sources is used, it becomes, from an availability calculation perspective, as a series-connected component because the source cluster is now a fundamental part for system operation such that if it is fails, the whole system fails. Hence, the microgrid availability cannot be higher than that of the only source cluster, which equals approximately 0.85 if five fuel cells with no redundancy are used, 0.96 if five microturbines with no redundancy are used, about 0.99 if five fuel cells with redundancy are used, or 0.9994 if five microturbines with redundancy are used. Clearly, microgrids cannot achieve adequate levels of availability without diverse power sources unless energy storage is used.

By showing that the influence of the circuit topology choices on U_{MG} is small, the previous quantitative analysis supports the choice for MIC as building blocks for microgrid architectures because it indicates that MIC represents a compromise solution between modularity, cost, and availability. Still, MIC architectures seem to be somewhat more sensitive to topology changes. Hence, it is relevant to briefly explore the characteristics of the MICs selected as benchmark topologies. Configurations with boost converters are marginally better than those with ISEPIC, and both of these topologies are better than the CSHB. As Fig. 13 suggests, the case with the worst availability performance is Configuration A with a CSHB, as exemplified in Fig. 10. Configuration C with boost converters is among the cases with the best performance, and its behavior is exemplified in Fig. 11. However, configurations with MI ISEPICs, such as Configuration F exemplified in Fig. 12 have an availability only marginally lower than that of the single-input or MI boost converters. Since the difference between the boost and the ISEPIC topologies is small; therefore, the choice between them may depend on other important criteria different from their influence on availability. For example, in steady state, the inputs-to-output voltages relationship for a two-input ISEPIC is given by [43]

$$V_{\mathrm{out}} = \frac{N_2(D_1 E_1 + (D_2 - D_1)E_2)}{N_1(1 - D_2)} \tag{10}$$

where N_1 and N_2 are the number of turns in the input and output sides, respectively, of the coupled inductor, V_{out} is the output voltage, E_1 is the highest input voltage, E_2 is the other input voltage, D_1 is the duty cycle of the switch of the leg, whose input voltage is E_1, and D_2 is the duty cycle of the other input leg. Equation (10) indicates that the ISEPIC can achieve higher conversion ratios than the boost, and is more suitable for tracking sources' maximum power point [43] because the output voltage can be higher or lower than the input voltage. The only disadvantage of the ISEPIC somewhat with respect to the boost is, in terms of power efficiency, particularly at high loads. The CSHB yields a slightly lower availability and is more costly than the other two topologies, but it can provide higher conversion ratios than the boost and may reach higher efficiencies than the ISEPIC. All of the three circuit topologies discussed herein have a current source interface suitable for all types of DG sources, including those, such as fuel cells, that require smooth currents. Due to this choice for equal input interface at all three benchmarking topologies, availability of sources, whose reliability data are based on performance degradation, such as in fuel cells, does not need to be modified in any case. However, a choice of converters with a voltage source interface, such as MI buck–boost [31] or the two-stage buck and boost [56], will require reducing the MUT of DG technologies that are negatively affected by switched output currents, such as fuel cells. The ISEPIC is once again used as an example of converters with current source interface. As Fig. 14 shows by testing a hardware prototype with $E_1 = 55.5$ V, $E_2 = 25$ V, $D_1 = 0.31$, $D_2 = 0.32$, $N_1 = 8$, $N_2 = 17$, $V_{\mathrm{out}} \approx 150$ V, and $P_{\mathrm{out}} = 217$ W—measuring an efficiency of about 92.5%—and a switching frequency of 80 kHz, the ISEPIC input currents are not switched. Contrary to the MI ISEPIC, there are preceding works presenting exper-
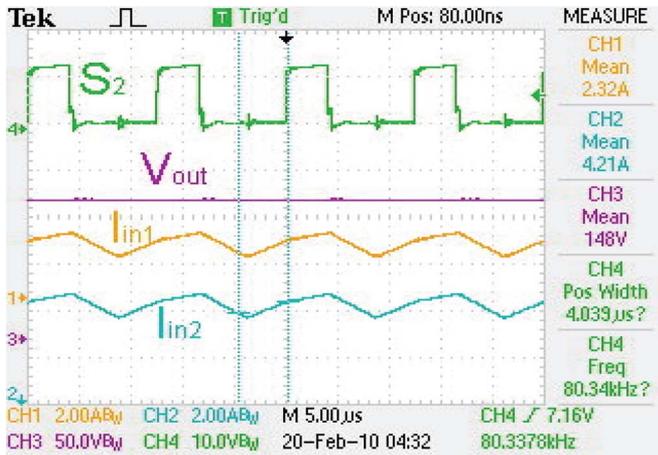
Fig. 14. Oscilloscope capture for a hardware prototype of a two-input ISEPIC. From top to bottom, the traces are: switching signal for the switch at the leg with the lowest input voltage (shown to provide an indication of the switching frequency), output voltage, input current at the leg with the highest voltage, and input current at the other leg.

imental behavior for the MI boost [42] and MI CSHB [57] and, thus, they are not shown in here. Experimental results for these three converters confirm that their behavior satisfy the conditions set forth when they were selected as benchmark topologies. They also confirm their suitability as an adequate compromise solution for microgrid source interfaces. Further analysis of the circuit operation is out of the scope of this paper. However, this discussion can be easily extended to other topologies not explicitly discussed here.

B. Comparison Between Microgrids and Conventional Standby Energy Systems

Since it has been claimed that one of the main applications of dc microgrids is in those cases, where they achieve higher availability than conventional backup energy systems, such as those found in telecommunications industry [32], [33], it is relevant to utilize the analytical approach presented here in order to quantitatively evaluate this assertion. While microgrids achieve high availability by diverse local power generation, conventional standby systems increase grid's availability through local energy storage in batteries—as it is going to be shown, standby diesel generators do not increase grid's availability by themselves to a sufficient level as required by critical loads. Hence, microgrids are true *power* plants, whereas conventional plants are instead backup *energy* systems. Although batteries are effective in order to increase availability, they are expensive and add important operational and maintenance issues, including limited cycling, effects of environmental conditions on life, and disposal. Hence, it is desirable to find an option, such as dc microgrids, that provides high availability without the need for energy storage. Energy storage that may be added to micro-grids as load following power buffers for sources with slow dynamic response is not considered in the analysis for two reasons: The first reason is that the function of power buffers is not to increase availability but rather to meet operational needs. The second reason is that stored energy in power buffers can feed the full load only for a relatively very short time.

Consider a conventional telecom plant such as the one in Fig. 15. From the analysis detailed in Appendix B, the availability of this plant can be obtained from the Markov diagram in Fig. 16. As the analysis in Appendix B yields, when continuous fuel supply is assumed for the genset, and an autonomy T_{BAT} time is considered for the batteries, the unavailability of a conventional standby energy plant is given by

$$U_{\mathrm{SYS}} = U_a e^{a_F T_{\mathrm{BAT}}} \tag{11}$$

where U_a is the sum of the steady-state probabilities of all the states representing a failed condition and $a_F = -(3\mu_{\mathrm{RS}} + \mu_{\mathrm{MP}} + \mu_{\mathrm{GS}})$, where μ_{RS}, μ_{MP}, and μ_{GS} are the failure rates of the rectifier system, the mains power, and the combined genset and its fuel supply, respectively. When a diesel fuel tank autonomy T_D is considered, the unavailability becomes

$$U_{\mathrm{SYS}} = P_{S_2} e^{a_D (T_D + T_{\mathrm{BAT}})} + U_a e^{a_F T_{\mathrm{BAT}}} \tag{12}$$

where P_{S2} is the state representing a condition when only the ac grid is in a failed state and $a_D = -(\lambda_{\mathrm{RS}} + \mu_{\mathrm{MP}} + \lambda_{\mathrm{GS}})$, where λ identify failure rates.

Without batteries, but with sufficiently long diesel storage—at least longer than the grid's MDT—the availability with respect to that of the grid can be improved by an order of magnitude, from 3-nines to 4-nines. With both T_{BAT} and T_D equal to 5 h, availability can be increased to 5-nines—still an order of magnitude lower than those obtained for most microgrid configurations in Table VIII—but such a long battery reserve time is typically very costly, particularly for high loads. Evidently, one alternative is to reduce T_{BAT} by increasing T_D, but with short battery reserves, in the order of an hour, and long and increasing fuel reserve times (longer than a day) availability increases marginally without barely exceeding 5-nines. When $T_D = 5$ h, an availability of 6-nines for energy backup plants can only be achieved with battery reserve times of 9 h. Without diesel generators, 5-nines availability requires about 9.5 h of battery energy storage, and 6-nines requires 14 h of energy storage. Therefore, this analysis quantitatively demonstrates that microgrids can achieve higher availabilities than conventional backup energy systems without the need for energy storage. Although microgrid's availability advantage is made at the expense of investing in local DG units, cost calculations indicate that for sites requiring over a hundred kilowatt, dc microgrids are still more economical than conventional backup plants [6]. These calculations involve adding the capital, installation, operations, and expected downtime cost evaluated over a given reference time span T_{ref}—e.g., 10 years because that is the typical life of lead-acid batteries. The proposed quantitative availability framework presented here is essential in order to calculate the expected downtime cost, which equals the unavailability multiplied by T_{ref} and by the unit cost of the downtime depending the application under evaluation [58]. Typically, a planning process intended for technology selection will calculate the total cost of ownership—i.e., total cost of the system under evaluation including downtime cost calculated for the entire lifespan of the system, from purchasing to decommissioning—and will select the option with the lowest cost. Hence, quantifying availability allows to evaluate, through downtime cost calculation, whether

it is worth the cost of achieving ultrahigh availability and if so, which way is more cost effective to achieve such an availability with a conventional energy plant or with a microgrid. If the answer is the latter option, the quantitative analysis answers the question of which microgrid configuration may be more suitable based on the expected cost. Thus, it might be of planning interest to evaluate if microgrids costs can be reduced by replacing source redundancy and even diversity by local energy storage.

C. Effects of Local Energy Storage on Microgrids Availability

From (11), the unavailability of a microgrid when batteries are added directly to its main bus is can be calculated from

$$U_{\mathrm{MG,ES}} = U_{\mathrm{MG}} e^{a_{\mathrm{MG}} T_{\mathrm{BAT}}}. \tag{13}$$

Since, each mcs can be related with a microgrid operational state, a lower bound for a_{MG} equals the sum of all transitions rates from each mcs directly into a working state, i.e., the sum of all repair rates from transitions leaving each mcs into a working state. From Table II and using Configuration B as an example, without redundancy in the sources

$$a_{\mathrm{MG}} = -\Bigg(\mu_{f1} + \mu_{f2} + N_S(\mu_{SC1} + \mu_{f1} + \mu_{SC2} + \mu_{f2})$$
$$+ \sum_{j=1}^{N_S} C_j^{N_S} C_{N_S-j+1}^{N_S}(j\mu_{SC1} + (N_S - j + 1)\mu_{SC2})\Bigg) \tag{14}$$

and with redundancy

$$a_{\mathrm{MG}} = -\Bigg(\mu_{f1} + \mu_{f2} + C_2^{N_S}(\mu_{SC1} + \mu_{f1} + \mu_{SC2} + \mu_{f2})$$
$$+ \sum_{j=2}^{N_S} C_j^{N_S} C_{N_S-j+2}^{N_S}(j\mu_{SC1} + (N_S - j + 2)\mu_{SC2})\Bigg) \tag{15}$$

where

$$\begin{cases} \mu_{SC1} = \dfrac{(\lambda_{S1} + \lambda_C)\mu_{S1}\mu_C}{\lambda_{S1}\mu_C + \lambda_C\mu_{S1} + \lambda_C\lambda_{S1}} \\[2ex] \mu_{SC1} = \dfrac{(\lambda_{S2} + \lambda_C)\mu_{S2}\mu_C}{\lambda_{S2}\mu_C + \lambda_C\mu_{S2} + \lambda_C\lambda_{S2}} \end{cases} \tag{16}$$

and λ and μ are the failure and repair rates, respectively, of fuel supplies (indicated by subindices $f1$ and $f2$), DG source units (indicated by subindices $S1$ and $S2$), and SIC (indicated by the subindex C). If microgrid costs are reduced by having only one DG unit in each of the two clusters, availabilities without added energy storage is about 4-nines. Calculations indicate that batteries connected directly to the main bus can increase availability up to 5-nines. Yet, for configurations A, B, D, and F significant energy storage, similar to that required in conventional backup energy systems, is needed in order to achieve such goal. This result is not surprising because the availability of DG units is poor compared to that of conventional grids, and because configurations C and E are the only two ones that can take advantage of having multiple converter modules in redundant arrangements

when the sources are in single not redundant configurations. Also, these calculations, although simple, only yield a lower bound for a_{MG}, and thus, an upper bound for T_{BAT}. However, once more DG units are added to each cluster, the required reserve time needed to reach 5-nines drops extremely fast.

D. Account for Discontinuous Fuel Supply in Availability Calculation Framework

One last point of interest in the proposed approach is to represent the fact that fuel supply for DG sources could not be continuous, but rather delivered at regular intervals and stored locally, i.e., distinguishing the case of natural gas supply, which is delivered continuously through a pipe, from the case in which liquid fuel is delivered at given intervals with a truck or some other transportation means. The proposed model here for such liquid fuel supply considers that the fuel supply process can be represented by two states. A working state S_{RF} when the system is being resupplied and fuel is flowing through the input nozzle leading to the fuel storage tank and a failed state S_F in which no fuel is flowing into the fuel storage tank input and the system is waiting to be resupplied. Hence, the MUT can be associated with the expected time it takes to refuel the system—for simplicity, this time is assumed here to be always constant—and the MDT can be associated with the time when the system is at a "waiting to be resupplied" state. Also for simplicity, it is assume that the transition rates between S_{RF} and S_F are constant. The model also considers that because of the fuel production, commercialization, and transportation processes, there is a $100 \times P_D\%$ chances that the system is not resupplied within T_R hours from the last time it was refueled. Here, the problem of representing the probability that the fuel system will transition from S_F to S_{RF} in [0,t) is analogous to that of finding the probability that a generic two-state system in its failed state is repaired—i.e., it transitions into the working state—in [0,t). Thus, from [35]

$$1 - P_D = 1 - e^{-\mu_{\mathrm{RF}} T_R} \tag{17}$$

where μ_{RF} is the transition rate from S_F to S_{RF}. Hence,

$$\mu_{\mathrm{RF}} = -\frac{1}{T_R}\ln(P_D). \tag{18}$$

Resupply unavailability $u_{F,\mathrm{RS}}$ is then,

$$u_{F,\mathrm{RS}} = \frac{\lambda_{\mathrm{RF}}}{\lambda_{\mathrm{RF}} + \mu_{\mathrm{RF}}} \tag{19}$$

where λ_{RF} is the inverse of the average expected time it takes to refuel the system. Thus, the unavailability u_f of locally stored fuel supply is as follows:

$$u_f = u_{F,\mathrm{RS}} e^{-\mu_{\mathrm{RF}} T_{fS}} \tag{20}$$

where T_{fS} is the fuel supply autonomy operating at the nominal load. As an example, consider a demanding situation, typically of what could be found after a natural disaster in which the microgrid needs to operate continuously with fuel for microturbines being resupplied by trucks reaching the site through heavily damaged roads. Hence, consider that $P_D = 0.2$, $T_R = 24$ h, and $\lambda_{\mathrm{RF}} = 1$ h. Then, $\mu_{\mathrm{RF}} = 6.7 \times 10^{-2}$ and $u_{F,\mathrm{RS}} =$

0.937. Thus, with these conditions, it requires a fuel tank capable of storing about a week of fuel in order to closely match 5-nines availability observed in continuous fuel supply, such as natural gas, and indicated in Table VII.

V. CONCLUSION

This paper presents a quantitative framework based on mcs theory that allows evaluating how dc–dc converters circuit topologies and system electrical architecture designs choices influence dc microgrids availability. The impact on availability of both conventional architectures with SICs and alternative configurations with MICs are evaluated. Calculations indicate that power architectures with MICs seem a good compromise approach suited for highly available microgrids because they enable source diversity—an essential need in order to achieve high availability—and achieve with fewer circuit components an availability only marginally below that of SIC modules. Configurations with center converters have availabilities of about 5-nines with redundant DG sources and 4-nines without redundancy. These values are of an order of magnitude worse than those calculated for modular SICs or MICs. Three converter topologies are considered as benchmarks because they are representative of other possible suitable alternatives: boost, ISEPIC, and CSHB. Although the ISEPIC has an availability only marginally below than the highest one achieved by the boost, the ISEPIC provides more operational flexibility because it can achieve high-voltage conversion ratios and track the entire output range of sources in search of a maximum power point.

Availability models for battery energy storage and discontinuous fuel delivery are included in the discussion. These models provide a way of quantifying the impact of locally added energy storage and of tradeoffs between battery storage and local fuel storage. These models served as a basis in order to compare microgrids with conventional backup energy systems and to demonstrate previously seemingly unproved claims that microgrids can achieve ultrahigh availabilities—higher than 5-nines—without local energy storage. Relevant applications for the proposed quantitative availability calculation method include risk assessments and microgrid controller development for optimal availability operation. Future research will study and develop such a controller, which would dynamically estimate microgrids availability in real time, typically intended to be used in smart-grid applications.

APPENDIX A

NOMENCLATURE USED IN TABLES

u_{f1} and u_{f2}: Fuel supply unavailability. In the studied cases, u_{f1} is the unavailability of the biofuel and u_{f2} is the unavailability of the natural gas.

u_{CC}: Center converters unavailability.

u_{S1} and u_{S2}: Unavailability of DG units. In the studied cases, u_{S1} is the unavailability of a microturbine unit and u_{S2} is the unavailability of a fuel cell unit.

N_S: Number of DG source units in each cluster. With $n + 1$ redundancy $N_S = n_S + 1$. Without redundancy $N_S = n_S$.

N_c: Number of converter modules. For configurations C and D, it is the number of SICs in each cluster. For configurations E and F is the number of MIC modules. With $n + 1$ redundancy, $N_C = n_C + 1$. Without redundancy $N_C = n_C$.

C_x^N: Number of combinations from a group of N equal components taken in groups of x. Since all components are equal and the order in which each component is picked is not important, then

$$C_x^N = \frac{N!}{x!(N-x)!}. \tag{21}$$

u_{SC1} and u_{SC2}: Unavailability of the series connection of a DG unit and a SIC. This unavailabilities equals

$$u_{SCj} = 1 - (1 - u_{Sj})(1 - u_C). \tag{22}$$

u_C: Unavailability of a SIC.

u_{sb1} and u_{sb2}: Unavailability of the series connection of a DG unit and a group of SICs in parallel. These unavailabilities equal

$$u_{Sbj} = 1 - (1 - u_{Sj})A_C \tag{23}$$

where

$$A_C = (1 - u_C)^{N_C} \quad \text{without redundancy} \tag{24}$$

$$A_C = N_C(1 - u_C)^{N_C - 1}u_C + (1 - u_C)^{N_C} \quad \text{with redundancy} \tag{25}$$

u_o: Unavailability of a MIC's output stage module.

u_i: Unavailability of an input module in a MIC.

u_{Si1} and u_{Si2}: Unavailability of the series connection of a DG unit and an input module from a MIC. This unavailability equals

$$u_{Sij} = 1 - (1 - u_{Sj})(1 - u_i). \tag{26}$$

NR: Not relevant. It applies when the redundancy policy of a given component does not affect the analysis.

APPENDIX B

STANDBY ENERGY PLANT AVAILABILITY CALCULATION

Consider a conventional telecom plant such as the one in Fig. 15. The availability of this plant can be obtained from the Markov diagram in Fig. 16. In this figure, each of the plant's states S_i is represented by a three-digit binary number in which the first digit represent the state of the rectifiers, the second digit represents the state of the ac mains, and the third digit represents the state of the genset. A "one" represents a failed state and a "zero" represents a working condition. Also in Fig. 16, λ_{GS} is the failure rate of the series combination of the generator set and diesel circuit, μ_{GS} is the combined genset and its fuel supply repair rate, ρ_{GS} is the genset failure-to-start probability, λ_{MP} is the mains power failure rate, and μ_{MP} is the mains power repair rate. The failure and repair rate λ_{RS} and μ_{RS} for the $n + 1$ redundant arrangement of rectifiers are as follows:
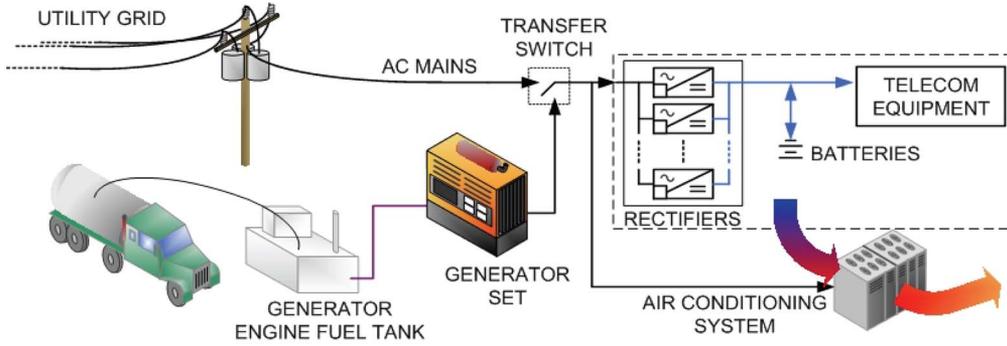
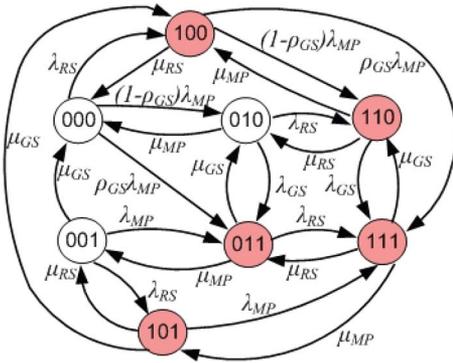Fig. 15. Typical telecom energy system elements and distribution architecture.

Fig. 16. Markov diagram for a conventional telecom energy system without considering the batteries.

$$\begin{cases} \lambda_{\mathrm{RS}} = \dfrac{n\lambda_r^2(n+1)}{(n+1)\lambda_r + \mu_r} \\[3mm] \mu_{\mathrm{RS}} = \dfrac{2\lambda_r^2\mu_r^n C_{n-1}^{n+1}}{\sum_{i=0}^{n-1} C_i^{n+1}\mu_r^i \lambda_r^{n+1-i}} \end{cases} \quad (27)$$

where λ_r and μ_r are the failure and repair rates of each rectifier, respectively.

Based on Fig. 16, a vector $\mathbf{P}(t)$ can be defined to represent the probability of being at any given state at time t. It can be obtained by solving the differential equation

$$\dot{\mathbf{P}}(t) = \mathbf{A}^T \mathbf{P}(t) \quad (28)$$

where $\mathbf{A}$ is indicated by (29) as shown at the bottom of this page, and $P_i(t)$ is the coordinate i of the vector $\mathbf{P}(t)$, such that the sum of all coordinates of $\mathbf{P}(t)$ equals 1 for all t. The probability $P_i(t)$ coincides with the probability P_{Sk} of being at the state $k = i - 1$ at time t. It is assumed that the genset is fueled by a continuous diesel delivery process (e.g., from a pipe coming directly from a diesel distribution center). All shaded states in Fig. 16 represent a failed condition for the energy system so they belong to the set F, whereas states S_0, S_1, and S_2 belong to the set W of the "working" states. The probability of plant failure is then,

$$P_{Pf}(t) = \sum_{S_i \in F} P_{S_i}(t) = 1 - \sum_{S_i \in W} P_{S_i}(t). \quad (30)$$

It can be shown [35], [59] that the probability density function $f_{PPf}(t)$ associated with the probability of leaving the set F after

$$\mathbf{A} = \begin{pmatrix}
-(\lambda_{\mathrm{MP}} + \lambda_{\mathrm{RS}}) & 0 & (1-\rho_{\mathrm{GS}})\lambda_{\mathrm{MP}} & \rho_{\mathrm{GS}}\lambda_{\mathrm{MP}} & \lambda_{\mathrm{RS}} \\
\mu_{\mathrm{GS}} & -(\mu_{\mathrm{GS}} + \lambda_{\mathrm{MP}} + \lambda_{\mathrm{RS}}) & 0 & \lambda_{\mathrm{MP}} & 0 \\
\mu_{\mathrm{MP}} & 0 & -(\lambda_{\mathrm{GS}} + \mu_{\mathrm{MP}} + \lambda_{\mathrm{RS}}) & \lambda_{\mathrm{GS}} & 0 \\
0 & \mu_{\mathrm{MP}} & \mu_{\mathrm{GS}} & -(\mu_{\mathrm{GS}} + \mu_{\mathrm{MP}} + \lambda_{\mathrm{RS}}) & 0 \\
\mu_{\mathrm{RS}} & 0 & 0 & 0 & -(\lambda_{\mathrm{MP}} + \mu_{\mathrm{RS}}) \\
0 & \mu_{\mathrm{RS}} & 0 & 0 & \mu_{\mathrm{GS}} \\
0 & 0 & \mu_{\mathrm{RS}} & 0 & \mu_{\mathrm{MP}} \\
0 & 0 & 0 & \mu_{\mathrm{RS}} & 0 \\
\end{pmatrix}$$

$$\begin{pmatrix}
0 & 0 & 0 \\
\lambda_{\mathrm{RS}} & 0 & 0 \\
0 & \lambda_{\mathrm{RS}} & 0 \\
0 & 0 & \lambda_{\mathrm{RS}} \\
0 & (1-\rho_{\mathrm{GS}})\lambda_{\mathrm{MP}} & \rho_{\mathrm{GS}}\lambda_{\mathrm{MP}} \\
-(\mu_{\mathrm{GS}} + \lambda_{\mathrm{MP}} + \mu_{\mathrm{RS}}) & 0 & \lambda_{\mathrm{MP}} \\
0 & -(\lambda_{\mathrm{GS}} + \mu_{\mathrm{MP}} + \mu_{\mathrm{RS}}) & \lambda_{\mathrm{GS}} \\
\mu_{\mathrm{MP}} & \mu_{\mathrm{GS}} & -(\mu_{\mathrm{GS}} + \mu_{\mathrm{MP}} + \mu_{\mathrm{RS}}) \\
\end{pmatrix}$$

$$(29)$$

being in the set from $t = 0$ and entering W at time $t + dt$ is as follows:

$$f_{Pf}(t) = -a_F e^{a_F t} \tag{31}$$

where a_F represent all the transition rates from F to W, i.e.,

$$a_F = -(3\mu_{\mathrm{RS}} + \mu_{\mathrm{MP}} + \mu_{\mathrm{GS}}). \tag{32}$$

Thus, the probability of leaving the set F after being in the set from $t = 0$ and entering W at a time longer than the battery backup time T_{BAT}—i.e., the probability of discharging the batteries—in such condition is as follows:

$$P_{\mathrm{BD}}(t > T_{\mathrm{BAT}}) = 1 - \int_{\tau=0}^{\tau=T_{\mathrm{BAT}}} f_{Pf}(\tau) d\tau$$

$$= 1 - \int_{\tau=0}^{\tau=T_{\mathrm{BAT}}} -a_F e^{a_F \tau} d\tau = e^{a_F T_{\mathrm{BAT}}}. \tag{33}$$

The outage probability is, then, the probability that the system failed at $t = 0$ and the batteries were discharged. If it is assumed that the system has been turned into operation at some time $T_{inic} \rightarrow -\infty$, then $P_{Pf}(t)$ equals the system unavailability U_a without batteries, and the outage probability is approximately the unavailability U_{SYS} of the eight-state system represented in Fig. 16 to which the effect of the energy stored in the batteries and expressed in (33) is added. Hence,

$$U_{\mathrm{SYS}} = U_a e^{a_F T_{\mathrm{BAT}}} \tag{34}$$

where U_a is the sum of the steady-state probabilities of all the states in F obtained by solving the linear algebraic system of equations yield by making the left side of (28) zero, and replacing one of the equations by

$$\sum_{i=0}^{7} P_{S_i} = 1. \tag{35}$$

Limited diesel storage and discontinuous fuel delivery can now be considered by assuming that the diesel tank is full each time before the system enters state S_2. More complex models involving refueling practices can be also considered, but they are out of the scope of this paper. Since the genset will only consume fuel when the system is at state S_2, then the new system unavailability without considering battery reserve time is as follows:

$$P_{Pf,LF}(t) = P_{S_2}(t > T_D) + \sum_{S_i \in F} P_{S_i}(t) \tag{36}$$

where T_D is the diesel reserve time yielded by the stored fuel at nominal operating conditions. Following a similar analysis from that included in (30)–(34) in reliability steady state

$$\lim_{t \to \infty} P_{S_2}(t > T_D) = P_{S_2} e^{a_D T_D} \tag{37}$$

where P_{S_2} is the steady-state probability of S_2 and a_D is the negative sum of the transition rate out of S_2. Thus,

$$a_D = -(\lambda_{\mathrm{RS}} + \mu_{\mathrm{MP}} + \lambda_{\mathrm{GS}}). \tag{38}$$

When batteries are considered in addition to limited fuel storage, the steady-state unavailability equals the probability of entering F at $t = 0$ and remaining there longer than T_{BAT} or of entering S_2 at $t = 0$ and remaining there longer than $T_D +$

T_{BAT}. Therefore, the new system unavailability with limited fuel storage and battery supply is as follows:

$$U_{\mathrm{SYS}} = P_{S_2} e^{a_D(T_D + T_{\mathrm{BAT}})} + U_a e^{a_F T_{\mathrm{BAT}}}. \tag{39}$$

REFERENCES

[1] D. Salomonsson, L. Söder, and A. Sannino, "An adaptive control system for a DC microgrid for data centers," *IEEE Trans. Ind. Appl.*, vol. 44, no. 6, pp. 1910–1917, Nov./Dec. 2008.

[2] A. Kwasinski and P. T. Krein, "A microgrid-based telecom power system using modular multiple-input dc-dc converters," in *Proc. INTELEC 2005*, pp. 515–520.

[3] H. Ikebe, "Power systems for telecommunications in the IT age," in *Proc. INTELEC*, 2003, pp. 1–8.

[4] D. G. Robinson, D. J. Arent, and L. Johnson, "Impact of distributed energy resources on the reliability of a critical telecommunications facility," Sandia Nat. Lab., Albuquerque, NM, and Nat. Renew. Energy Lab., Golden, CO, Rep. SAND2006–1277, NREL/TP-620–39561, Mar. 2006.

[5] A. Kwasinski, "Analysis of vulnerabilities of telecommunication systems to natural disasters," in *Proc. IEEE Syst. Conf.*, 2010, pp. 359–364.

[6] A. Kwasinski and P. T. Krein, "Optimal configuration analysis of a microgrid-based telecom power system," in *Proc. INTELEC 2006*, pp. 602–609.

[7] W. Allen, D. Fletcher, and K. Fellhoelter, "Securing critical information and communication infrastructures through electric power grid independence," in *Proc. INTELEC*, 2003, pp. 170–177.

[8] W. Allen and S. Natale, "Achieving ultra-high system availability in a battery-less –48VDC power plant," in *Proc. INTELEC*, 2002, pp. 287–294.

[9] A. Prasai, A Paquette, Y. Du, R. Harley, and D. Divan, "Minimizing emissions in microgrids while meeting reliability and power quality objectives," in *Proc. IPEC 2010*, pp. 726–733.

[10] F. A. Mohamed and H. N. Koivo, "MicroGrid online management and balancing using multiobjective optimization," in *Proc. IEEE Power Tech.*, 2007, pp. 639–644.

[11] C. Marnay, G. Venkataramanan, M. Stadler, A. Siddiqui, R. Firestone, and B. Chandran, "Optimal technology selection and operation of commercial-building microgrids," *IEEE Trans. Power Syst.* vol. 23, no. 3, pp. 975–982, Aug. 2008.

[12] A. P. Agalgaonkar, S. V. Kulkarni, and S. A. Khaparde, "Evaluation of configuration plans for DGs in developing countries using advanced planning techniques," *IEEE Trans. Power Syst.*, vol. 21, no. 2, pp. 973–981, May 2006.

[13] C. A. Hernandez-Aramburo, T. C. Green, and N. Mugniot, "Fuel consumption minimization of a microgrid," *IEEE Trans. Ind. Appl.*, vol. 41, no. 3, pp. 673–681, May/Jun. 2005.

[14] E. Barklund, N. Pogaku, M. Prodanovic, C. Hernandez-Aramburo, and T. C. Green, "Energy management in autonomous microgrid using stability-constrained droop control of inverters," *IEEE Trans. Power Electron.*, vol. 23, no. 5, pp. 2346–2352, Sep. 2008.

[15] Y. W. Li and C.-N. Kao, "An accurate power control strategy for power-electronics-interfaced distributed generation units operating in a low-voltage multibus microgrid," *IEEE Trans. Power Electron.*, vol. 24, no. 12, pp. 2977–2988, Dec. 2009.

[16] Y. A.-R. I. Mohamed and E. F. El-Saadany, "Adaptive decentralized droop controller to preserve power sharing stability of paralleled inverters in distributed generation microgrids," *IEEE Trans. Power Electron.*, vol. 23, no. 6, pp. 2806–2816, Nov. 2008.

[17] J. Kim, J. Lee, and K. Nam, "Inverter-based local AC bus voltage control utilizing two DOF control," *IEEE Trans. Power Electron.*, vol. 23, no. 3, pp. 1288–1298, May 2008.

[18] B. Kroposki, C. Pink, R. DeBlasio, H. Thomas, M. Simoes, and P. K. Sen, "Benefits of power electronic interfaces for distributed energy systems," *IEEE Trans. Energy Convers.*, vol. 25, no. 3, pp. 901–908, Sep. 2010.

[19] H. Nikkhajoei and R. H. Lasseter, "Distributed generation interface to the CERTS microgrid," *IEEE Trans. Power Del.*, vol. 24, no. 3, pp. 1598–1608, Jul. 2009.

[20] I.-S. Bae and J.-O Kim, "Reliability evaluation of customers in a microgrid," *IEEE Trans. Power Syst.*, vol. 23, no. 3, pp. 1416–1422, Aug. 2008.

[21] A. K. Basu, S. Chowdhury, and S. P. Chowdhury, "Impact of strategic deployment of CHP-based DERs on microgrid reliability," *IEEE Trans. Power Del.*, vol. 25, no. 3, pp. 1697–1705, Jul. 2010.

[22] P. S. Patra, J. Mitra, and S. J. Ranade, "Microgrid architecture: A reliability constrained approach," in *Proc. IEEE Power Eng. Soc. Meeting*, 2005, vol. 3, pp. 2372–2377.

[23] J. Mitra, S. B. Patra, and S. J. Ranade, "Reliability stipulated microgrid architecture using particle swarm optimization," in *Proc. PMAPS*, 2006, pp. 1–7.

[24] A. K. Basu, S. P. Chowdhury, S. Chowdhury, S. D. Ray, and P. A. Crossley, "Reliability study of a micro-grid power system," in *Proc. UPEC 2008*, pp. 1–4.

[25] J. W. Kimball, B. T. Kuhn, and R. S. Balog, "A system design approach for unattended solar energy harvesting supply," *IEEE Trans. Power Electron.*, vol. 24, no. 2, pp. 952–962, Apr. 2009.

[26] S. H. Choung and A. Kwasinski, "Multiple-input DC-DC converter topologies comparison," in *Proc. IECON 2008*, pp. 2359–2364.

[27] A. Kwasinski and P. T. Krein, "Multiple-input dc-dc converters to enhance local availability in grids using distributed generation resources," in *Proc. Rec. APEC 2007*, pp. 1657–1663.

[28] F. Blaabjerg, Z. Chen, and S. B. Kjaer, "Power electronics as efficient interface in dispersed power generation systems," *IEEE Trans. Power Electron.*, vol. 19, no. 5, pp. 1184–1194, Sep. 2004.

[29] Y. Ito, Y Zhongqing, and H. Akagi, "DC microgrid based distribution power generation system," in *Proc. Power Electron. Motion Control Conf.*, 2004, vol. 3, pp. 1740–1745.

[30] A. Khaligh, "A multiple-input dc-dc positive buck-boost converter topology," in *Proc. APEC 2008*, pp. 1522–1526.

[31] B. Dobbs and P. Chapman, "A multiple-input dc-dc converter topology," *IEEE Power Electron. Lett.*, vol. 1, no. 1, pp. 6–9, Mar. 2003.

[32] S. R. Ali, *Digital Switching Systems. System Reliability and Analysis*. New York, NY: Mc Graw-Hill, 1998.

[33] D. R. Kuhn, "Sources of failure in the public switched telephone network," *Computer*, vol. 30, pp. 31–36, Apr. 1997.

[34] A. Kwasinski, "Technology planning for electric power supply in critical events considering a bulk grid, backup power plants, and microgrids," *IEEE Syst. J.*, vol. 4, no. 2, pp. 167–178, Jun. 2010.

[35] A. Villemeur, *Reliability, Availability, Maintainability, and safety assessment. Volume 1, Methods and Techniques*. West Sussex, Great Britain: Wiley, 1992.

[36] Y. Chen, D. K.-W. Cheng, and Y.-S. Lee, "A hot-swap solution for paralleled power modules by using current-sharing interface circuits," *IEEE Trans. Power Electron.*, vol. 21, no. 6, pp. 1564–1571, Nov. 2006.

[37] V. Choudhary, E. Ledezma, R. Ayyanar, and R. M. Button, "Fault tolerant circuit topology and control method for input-series and output-parallel modular DC-DC converters," *IEEE Trans. Power Electron.*, vol. 23, no. 1, pp. 402–411, Jan. 2008.

[38] A. Kwasinski, "Identification of feasible topologies for multiple-input dc-dc converters," *IEEE Trans. Power Electron.*, vol. 24, no. 3, pp. 856–861, Mar. 2009.

[39] Y. -C. Liu and Y. -M. Chen, "A systematic approach to synthesizing multi-input DC/DC converters," in *Proc. Rec. IEEE PESC*, 2007, pp. 2626–2632.

[40] H. Tao, A. Kotsopoulos, J. L. Duarte, and M. A. M. Hendrix, "Family of multiport bidirectional dc-dc converters," *IEE Proc. Electron. Power Appl.*, vol. 153, no. 3, pp. 451–458, May 2006.

[41] Y. Li, X. Ruan, D. Yang, F Liu, and C. K. Tse, "Synthesis of multiple-input DC/DC converters," *IEEE Trans. Power Electron.*, vol. 25, no. 9, pp. 2372–2385, Sep. 2010.

[42] A. Di Napoli, F. Crescimbini, L. Solero, F. Caricchi, and F. G. Capponi, "Multiple-input dc-dc power converter for power-flow management in hybrid vehicles," in *Proc. IEEE Ind. Appl. Conf.*, 2002, pp. 1578–1585.

[43] J. Song and A. Kwasinski, "Analysis of the effects of duty cycle constraints in multiple-input converters for photovoltaic applications," in *Proc. INTELEC 2009*, p. 5.

[44] R. Balog, L. Cerven, N. Schweigert, N. Schroeder, J. Woodward, B. Mathis, and P. Krein, "Low-cost 10 kW inverter system for fuel cell interfacing based on PWM cycloconverter," Future Energy Challenge 2001 Final Rep., Online [Available] http://www.energychallenge.org/2001Reports/Illinois.pdf

[45] L. Palma and P. N. Enjeti, "A modular fuel cell, modular DC–DC converter concept for high performance and enhanced reliability," *IEEE Trans. Power Electron.*, vol. 24, no. 6, pp. 1437–1443, Jun. 2009.

[46] C. Chien-Liang Chen, W. Yubin, L. Jih-Sheng, L. Yuang-Shung, and D. Martin, Design of parallel inverters for smooth mode transfer microgrid applications," *IEEE Trans. Power Electron.*, vol. 25, no. 1, pp. 6–15, Jan. 2010.

[47] L. L. Bucciarelli, "Estimating loss-of-power probabilities of stand-alone photovoltaic solar energy systems," *Solar Energy*, vol. 32, no. 2, pp. 205–209, 1984.

[48] J. Kippen, "Evaluating the reliability of DC/DC converters," Internet: Online [Available] http://www.astec.com/whitepaper/dcdc/WP-POL%20Purchase%20 or%20Design%2006%20ok.pdf, Sep. 2003 [Nov. 30, 2006].

[49] *Reliability Prediction of Electronic Equipment*, U. S. Department of Defense, Pentagon, Washington, DC, MIL-HDBK-217, Feb. 1995.

[50] M. Fowler, "Degradation and reliability modeling of polymer electrolyte membrane (PEM) fuel cells," (Dec. 2010). Online [Available] Internet: http://chemeng.uwaterloo.ca/faculty/Mike%20Fowler%20-%20personal%20web%20pages/degradation.pdf

[51] C. A. Smith, M. D. Donovan, and M. J. Bartos, "Reliability survey of 600 to 1800 kW diesel and gas-turbine generating units," *IEEE Trans. Ind. Appl.*, vol. 26, no. 4, pp. 741–755, Jul./Aug. 1990.

[52] P. S. Hale and R. G. Arno, "Survey of reliability and availability information for power distribution, power generation, and HVAC components for commercial, industrial, and utility installations," in *Proc. Rec. Ind. Commercial Power Systems Tech. Conf.*, 2000, pp. 31–54.

[53] K. N. Choma and M. Etezadi-Amoli, "The application of a DSTATCOM to an industrial facility," in *Proc. IEEE Power Eng. Soc. Winter Meeting*, 2002, vol. 2, pp. 725–728.

[54] F. Bodi, "Practical reliability modeling of complex telecommunications services," in *Proc. INTELEC*, 1993, vol. 1, pp. 28–33.

[55] C. Marnay, "Microgrids and heterogeneous security, quality, reliability, and availability," in *Proc PCC 2007*, pp. 629–634.

[56] A. Khaligh, C. Jian, and Y-J Lee, "A multiple-input DC–DC converter topology," *IEEE Trans Power Electron.*, vol. 24, no. 3, pp. 862–868, Mar. 2009.

[57] H. Tao, A. Kotsopoulos, J. L. Duarte, and M. A. M. Hendrix, "Multi-input bidirectional DC-DC converter combining DC-link and magnetic-coupling for fuel cell systems," in *Proc. IEEE Ind. Appl. Conf.*, 2005, vol. 3, pp. 2021–2028.

[58] S. Roy, "Reliability considerations for data centers power architectures," in *Proc. Rec. INTELEC 2001*, pp. 406–411.

[59] R. Billinton and R. N. Allan, *Reliability Evaluation of Power Systems*. New York, NY: Plenum Press, 1984.

Alexis Kwasinski (S'03–M'07) received the B.S. degree in electrical engineering from the Buenos Aires Institute of Technology (ITBA), Buenos Aires, Argentina, in 1993, the Graduate specialization degree in telecommunications from the University of Buenos Aires, Buenos Aires, in 1997, and the M.S. and Ph.D. degrees in electrical engineering from the University of Illinois at Urbana-Champaign, in 2005 and 2007, respectively.

From 1993 to 1997, he was with Telefónica of Argentina for four years, where he was involved in designing and planning telephony outside plant networks. Then, he worked for five years for Lucent Technologies Power Systems (later Tyco Electronics Power Systems) as a Technical Support Engineer and Sales Technical Consultant in Latin America. For three years, he was also a Part-Time Instructor In-Charge of ITBA's Telecommunications Laboratory. He is currently an Assistant Professor in the Department of Electrical and Computer Engineering, University of Texas at Austin. His research interests include power electronics, distributed generation, renewable and alternative energy, and analysis of the impact of extreme events on critical power infrastructure, which included performing damage assessments after several natural disasters, such as hurricanes Katrina (2005) and Ike (2008), and the 2010 Maule, Chile Earthquake.

Dr. Kwasinski is also an active participant in Austin's smart grid initiative: the Pecan Street Project. During 1994–1995, he was a member of the Executive Committee of the Argentine Electrotechnical Association. In 2005, he was awarded the Joseph J. Suozzi INTELEC Fellowship. In 2007, he was the recipient of the Best Technical Paper Award at INTELEC. In 2009, he was the recipient of the National Science Foundation CAREER award. He is also an Associate Editor for the IEEE TRANSACTIONS ON ENERGY CONVERSION.